Master Thesis

Department of Technology and Software

Major: Data Science

Ajetunmobi Oluwasegun

Matriculation Number: 49084524

Supervisor: Prof. Dr. Talha Ali Khan

Co-supervisor: Prof. Dr. Syed Arslan

February 28, 2024

Statutory Declaration

I hereby declare that this master thesis is completely self-created and that sources and means, both from original publications and their use in the text, have been declared for use in this academic work. I have done my best to mark and separate from the text all the literature and other aids used when producing this academic work, either literally or in content. I am aware that if found guilty of violating this regulation, my thesis may not be accepted.

....
Sign Place, Date

Abstract

The extraction of the parameters of solar photovoltaic models is an optimization problem which is nonlinear, multivariable and and complex. In this thesis, six modifications were made to the Improved Whale Optimization Algorithm (IWOA) in order to improve the efficacy of the algorithm. These modifications adopt the properties of algebraic and transcendental functions such that the algorithm's balance between exploration and exploitation can be balanced measurably. Ten experiments were carried out to test each of the six modifications on ten benchmark functions. The results were plotted and statistically analyzed to provide a performance overview. The experimental results demonstrated that the modifications are feasible improvements of the IWOA.

Contents

Nomenclature

A	Current
a	Linearly decreasing parameter
b	constant
$I - V$	Current - Voltage
I_t	Output (Terminal) Current (A)
I_{ph}	Photo-generated Current (A)
I_{sd}	Shunt diode current (A)
I_{sh}	Shunt resistor current (A)
k	Boltzmann constant ($1.3806503 \times 10^{-23} J/K$)
k	Temperature
l, p	Random real numbers $\in (0, 1)$
n	Ideality factor of the diode
P	Power
q	Charge magnitude of an electron ($1.60217646 \times 10^{-19} C$)
R_s	Series resistance (Ω)
R_{sh}	Shunt resistance (Ω)
t	current iteration
V	Voltage
V_t	Terminal Voltage (V)

List of Abbreviations

ABC Artificial Bee Colony

CSO Cat Swarm Optimization

DD Double Diode

EA Evolutionary Algorithm

FPOA Flower Pollination Optimization Algorithm

ICA Imperialist Competitive Algorithm

IWOA Improved Whale Optimization Algorithm

MAKWO Modified Artificial Killer Whale Optimization

MPPT Maximum Power Point Tracking

MPP Maximum Power Point

PV Photo Voltaic

RMSE Root Mean Square Error

SA Simulated Annealing

SC Solar Cell

SD Single Diode

STC Standard Test Condition

TD Triple Diode

WOA Whale Optimization Algorithm

List of Figures

List of Tables

Chapter 1

Introduction

In recent decades, the rising population has warranted an up rise in the the demand for electrical energy. This increasing demand for this energy calls for a sustainable solution which will be in a position to cater for the ever-increasing world's population without incurring a lot of environmental damage. Coupled with the rapid depletion of non-renewable energy resources the urgency of developing renewable energy sources has been highlighted among researchers and leading economies. Among these alternatives, solar energy has emerged as a mature and promising option due to its potential to generate electricity and thermal energy without water or fuel consumption, while also minimizing pollution and contributing significantly to ecological improvement [48].

Solar energy stands out as a strong contender among the proposed alternatives and solutions. The sun represents an abundant source of energy, and harnessing its power can address the escalating energy demands while reducing the adverse environmental effects associated with conventional energy sources [48]. Solar energy is particularly effective in power generation, especially through the use of photovoltaic (PV) technology [22, 28, 77]. Photovoltaic panels, which rely on solar cells (SC), efficiently convert sunlight into electricity in an environmentally friendly and renewable manner. This aspect of solar energy production makes it an attractive option for sustainable energy generation [15].

However, it is important to acknowledge that the procurement and installa-

tion of PV systems can be relatively costly, particularly in regions where solar energy adoption is in its early stages. Despite the sustainability of PV modules, some energy efficiency challenges cannot be overlooked. Researchers have identified several critical issues that warrant further research and development in solar energy, including cost barriers, technological limitations, and regional disparities [60, 47, 24]. These challenges, while posing obstacles, also present opportunities for advancing the efficiency, affordability, and global accessibility of photovoltaic energy [15].

Furthermore, it is imperative to have accurate modelling of the photovoltaic (PV) cell to optimize the effectiveness and maximize the energy output of solar technologies. The nonlinearity in the current-voltage (I-V) behaviour of PV systems often induces difficulties in parameter identification. Hence advanced techniques are inevitable to precisely simulate, performance assessment, and design optimization. Determining key parameters accurately is pivotal to the complex process of modelling PV cells [102]. The complexity in the modelling process arises from the nonlinear I-V curve and the effects associated with the interaction of PV systems with peculiar facts. To determine such factors as semiconductor materials and electrical characteristics about the interaction of a system with sunlight makes the entire phenomenon utterly complex. Therefore the behavior of PV cells could not be correctly represented by traditional linear models. To cope with such challenges, therefore, the researchers and engineers developed advanced algorithms and simulation tools. The tools exposed and solved issues that included temperature variation, shadowing, and array configurations amongst others; hence a correct model of PV cells. This precision extends beyond simulation, aiding in performance evaluation and design optimization.

In the recent past, the strategies of determining the electrical model parameters have become prominent among the meta-heuristic algorithms due to their capability of handling linear and complex nonlinear optimization problems without being bound by accurate mathematical model requirements. This thus reduces computational burdens greatly and hence has been applied widely in PV cell parameter identification [102]. One of the more recent and interesting meta-heuristic algorithms developed is the Whale Optimization Algorithm. Inspired by the behaviour of humpback whales, it employs a unique hunting strategy characterized by the use of bubbles to create a net around the prospective prey, combining it with random search methods to explore the solution space. This approach although potent, has some limitations as it might not thoroughly examine the entire solution space leading to stagnation as it has no way to reassess and escape local minima after falling

into it [59]. This makes it a critical consideration for its application in PV parameter estimation.

1.1 Thesis Objectives

This thesis proposes modifications to a key parameter in the Improved Whale Optimization Algorithm, by leveraging the defining properties of some mathematical functions. The motivation behind this is to improve the case effectiveness of the IWOA in estimating the parameters of Triple-Diode Photovoltaic Cells and in turn, improve the application flexibility of the algorithm for other similar problems. With that said, this thesis will have three main objectives:

1. Conduct an extensive study of photovoltaic parameter estimation, the whale optimization algorithm and its related improvements
2. Modify the Improved Whale Optimization [100] algorithm for increased robustness and search space potency.
3. Analyze the modifications and test them with unimodal and multimodal benchmark functions to determine the most feasible.
4. Use the most effective modification to estimate the parameters of a triple-diode photovoltaic cell.

1.2 Thesis Contributions

The research written in this thesis contributes to solar energy optimization or triple diode PV systems in the following ways:

1. Modification of the IWOA in novel ways to improve the robustness and exploration capabilities of the algorithm
2. Explanation of the modification variations, their mathematical structure and functionalities through various means.

3. Potential impact on other algorithms via possible translational applications to other use cases

Chapter 2

Literature Review

This chapter reviews current and recent literature reviewed and explored during the writing of this thesis. The literature covered concepts such as photovoltaic modules, PV cell operation, the importance of parameter estimation, the basic principles of parameter extraction, existing numerical estimation techniques; SD, DD and TD specific techniques, metaheuristic algorithms, the WOA and IWOA and its performance, as well as the gaps that motivated the thesis. A particular focus will be made on the IWOA whose improvement in the context of photovoltaics will be the primary objective of this thesis. When reviewing associated literature, various databases such as Google Scholar, IEEE Explore, ScienceDirect, JSTOR, Directory of Open Access Journals (DOAJ), JSTOR and Elsevier were queried using relevant keywords associated with concepts relevant to the research.

Solar energy is undeniably the cleanest and most abundant energy source known to mankind. To harness this power source "solar cell modules which are plastic strips coated with thin films of photovoltaic silicon that collect solar energy for instant conversion into electricity" [70] were invented.

The photovoltaic module includes a non-conductive frame, a back sheet layer, a transparent support layer on the top, and a photovoltaic layer disposed between the back sheet and the transparent support layer. The photovoltaic region contains a consolidation of photovoltaic cells connected in scientifically coherent ways to foster current flow [41]. A non-conductive frame is made of at least one element selected from the group of a polymer element and

a polymer element exposed to radiation, such that an element of the frame is adapted to contact a portion of the back sheet layer and the transparent upper support layer. The four layers then undergo a structural amalgamation to yield the photovoltaic module [41]. Following years of research, a wide range of various modules such as the mono-crystalline, poly-crystalline, thin-film, bi facial, building-integrated PVs, concentrated PVs, amorphous silicon and others, were developed. As a result of these developments, the use of Photovoltaics in power generation has experienced commercial growth as they can be assimilated for use, into the walls of building structures, even replacing glass windows with translucent crystalline solar-panel systems[75]. However, the maximum conversion efficiency of solar cells is not very impressive and has been limited to percentages between 34 to less than about 45 for single material and more efficient cells respectively [6]. Even though this limit was recently pushed to about 48% for high-performance solar cells [101], the material requirements make it expensive and not commercially available to everyone.

This unsatisfactory conversion rate is evidenced by the Maximum Power Point (MPP) of each module and consequently necessitates the need to develop ways to improve conversion efficiency in ways that do not completely depend on expensive manufacturing processes and materials that will make the solar cell expensive and out of reach to the common man. To improve the conversion efficacy of a photo voltaic system, it has to be function at its Maximum Power Point (MPP) [66]. To predict the MPP of the PV system before investments are made, analytic [85] and numerical results have shown that there needs to be more accurate component information about the parameters responsible for the value of the MPP. [90]. If this is possible, the MPP can be pre-determined based on estimated parameters so that adjustments can be made to subsequently improve the PV module and its conversion efficiency. While some of the values of the parameters that combine to yield the MPP are provided in the manufacturer's data-sheet, there are still unknown parameters like the empirical values of the shunt resistance, series resistance, the diode ideality factor, photo-generated current and diode saturation current, which must be extracted to effectively model a PV system [14].

The literature revealed that to extract these parameters reliably, the analysis results of whatever parameter extraction technique must be compared with monitored values to ensure validity [91]. Among these monitored values research has been carried out to extract parameters based on two key factors: the I-V characteristics [67, 5] and the instantaneous environmental or weather

condition of the PV module [40, 55].

Research has been done to investigate the impact of environmental factors like irradiance, wind speed, incident angle and temperature [93, 25, 62, 61]

The better temperature dependence is represented during parameter estimation, the more practical we can expect the module to be, under varying physical conditions. However, to measure the correctness of our estimated parameters, researchers adopted various tools. One of which is the Root Mean Square Error (RMSE) which allows us to get an acceptable accuracy of the estimated module coefficients in comparison to the experimental values [71].

The triple-diode model comprises three diode components for different types of recombination processes or loss mechanisms existing in solar cells. Ideally, one diode represents an ideal p-n junction, another diode describes recombination in the depletion region and the third could represent surface or space charge region recombination. This model produces a more sweeping outlook on the nature of the cell, considering cases where part of the cell was shaded or under low light [84]. Even though the triple diode model is primarily used for research and simulation, it still gives a good avenue for researchers to improve the design and efficiency of both solar cells and extraction techniques [4].

Consequently, an intelligent Maximum Power Point Tracking (MPPT) controller was designed for the practical case of solar PV systems with moderate size to aid engineers and researchers in developing a very accurate model using only three diodes and to exactly forecast the performance of PV modules in a more predictive manner [11].

Accurate parameter estimation of solar cells is vital to assess and predict the performance of photovoltaic energy systems [46]. With the consistently upward growth trend of solar energy applications, the challenge of parameter estimation of PV cells has drawn the attention of researchers and industrialists quite significantly[18, 1]. Various techniques have been adopted in the literature to estimate the parameters of PV modules. An approach to the single-diode equivalent circuit model estimation was proposed [57], which is based on "an analysis of the characteristics of the solar panel supplied by the manufacturer" [57]. The method combines the solution of a system of algebraic equations with an optimization algorithm for extracting the seven photovoltaic module parameters of the single-diode lumped circuit model

[19]. Following this approach, This approach was consequently improved to demonstrate 0.1%–0.5% estimation precision when the Standard Operation Conditions data from the manufacturers' data sheets are employed [58]. Cell modelling and model parameters estimation techniques for photovoltaic simulator application were studied [17, 99]. Analytical and soft computing approaches are covered in detail. The Gauss-Seidel iterative scheme was adopted to iteratively estimate the parameters of five mathematical models of the SD PV module under varying conditions. Each model was differentiated by the combination of the photocurrent and reverse saturation current. It was shown that the iterative method engaged was suitable for this [29]. Many optimization methods have also been used to estimate the parameters of Double Diode models as well. The Newton-Raphson method was also engaged to estimate the parameters of double diode PV cells [73]

A reliable methodology based on an imperialist competitive algorithm (ICA) for estimating the optimal parameters of a photovoltaic (PV) generating unit was presented [30, 105]. The constrained objective function proposed by the literature was derived from the voltage-power curve of the PV system which is characterized by a peculiar maximum power point (MPP) [105].

A detailed review of the applications of various metaheuristic algorithms to PV systems in previous years has been comprehensively detailed in a paper by Oliva et al. [74] and Jordehi [45]. Evolutionary Algorithms (EA) were also considered while the literature was explored. These adaptive techniques are based on natural or biological evolution and natural selection. Specifically, they engage a randomized process of selection, mutation and recombination to arrive at a globally optimal solution [12]. Due to its robust possibility of applications to research cases, EAs have become an important optimization and search technique in recent decades [96]. Two variants of EAs were considered during the research phase of this thesis: Differential Evolution [33] and Genetic Algorithm [9]. They are effective at estimating parameters but only when all the parameters are tuned to fit the environmental context of the module [9]. Simulated Annealing (SA) was used to estimate the parameters of a double diode PV module. Inspired by the concept of annealing in metallurgy, it transposes ideas like entropy and thermodynamic free energy to create a probabilistic method for approximating the global optima of a search space [39]. In this technique, the parameters are first extracted using conventional methods. Then the uncertainties of each parameter are computed to compact the search space of the parameters and then the immediate values are determined using the results of the first two considerations. This process was confirmed to be quite effective when compared against other

established algorithms [63].

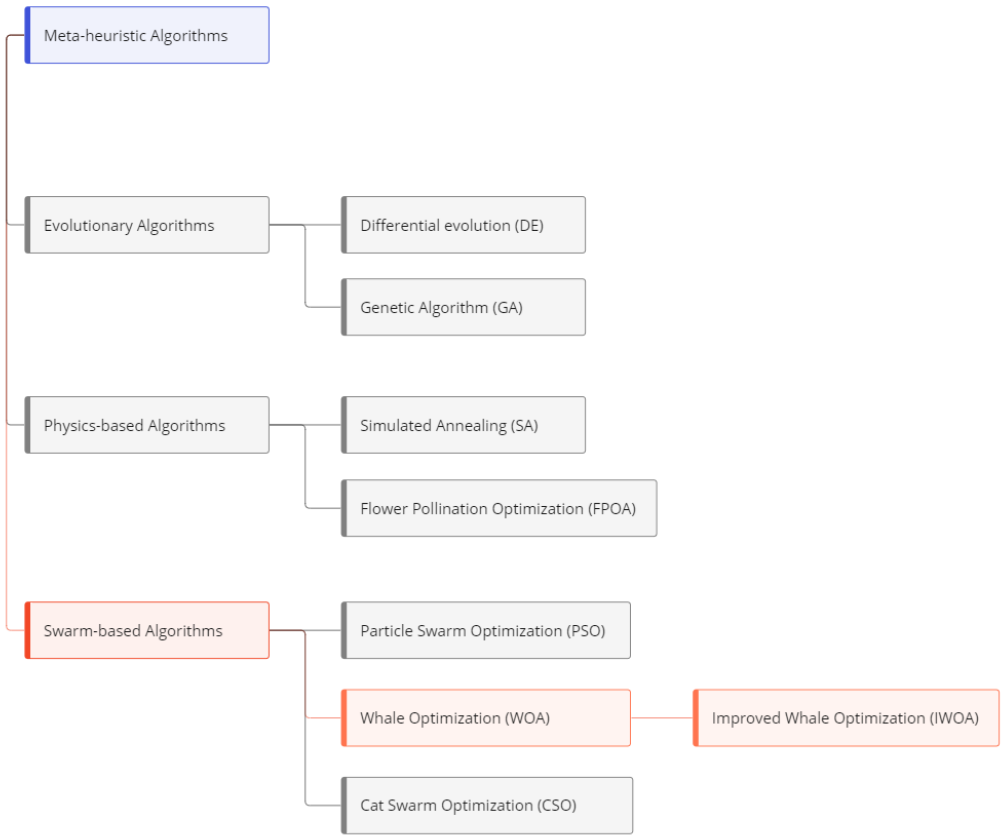

Figure 2.1: Classification of reviewed metaheuristic algorithms

Researchers developed the Flower Pollination Optimization Algorithm (FPOA) for parameter estimation in PV cells. This method draws from the behaviour of bees when seeking out flowers for nectar harvesting. In this scenario, the flower positions are considered to be the possible solution locations in the search space, while the amount of nectar they hold becomes the objective function to be maximized [104]. This method was applied to a given TD PV model and was shown to provide a greater performance quality than when applied on SD and DD models, which execute the local and global search protocol within a single jump[13]. Swarm intelligence has been engaged in the extraction of parameters. A frequently occurring example of this is the Particle Swarm Optimization (PSO) which is popularly used for other research cases. The PSO simply initializes particle vectors as search agents in a closed

domain which randomly search for the global best solution by adjusting their direction and path relative to the best-performing particle in each iterative step [98]. The PSO was used to align the computed I-V determinants of the PV cells to the experimentally obtained ones [53]. Following this, improvements such as the Fractional Order Darwinian Particle Swarm Optimization have been developed and applied to DD models successfully[65].

The Cat Swarm Optimization (CSO) algorithm has been posited as a way to estimate the unknown parameters of single and double-diode models [35]. The CSO algorithm is induced by the behaviour of cats searching for food as a group and was shown to be an effective tool in optimizing the parameters of SC models.

The Whale Optimization Algorithm (WOA) is a relatively new meta-heuristic optimization algorithm which mimics the helix-shaped hunting behaviour of humpback whales [82, 105] and has been shown to outperform popular choices such as the PSO [50]. It was proposed to analyze and model the PV system while considering both series and shunt resistances to track the MPP of the system [54]. The Modified Artificial Killer Whale Optimization (MAKWO) [87] introduced a modified algorithm to track a photovoltaic module's maximum power point under partially shaded conditions [36]. Popular and proven methods for maximum power point tracking and optimizations have been compared with a proposed MAKWO algorithm like a Modified Artificial Wolf Pack (MAWP) algorithm [37, 10], an artificial bee colony (ABC) [49, 10], and PSO [10]. A comparison has been drawn using four such compared results, and at last, pronounce the superiority of the MAKWO algorithm over all existing techniques of MPPT [36]. While effective in a general myriad of cases, the WOA was noticed to stagnate when handling multimodal problems and converge at local minima. This prompted the development of the Improved Whale Optimization Algorithm (IWOA) which proposed two strategies for prey position acquisition to balance local and global exploitation and exploration respectively [100]. It was shown that the IWOA was better than the original WOA. Parameter adaptive methods to effectively adjust the coefficient A to enhance the performance of IWOA were remarked as an opportunity for further research [100].

Chapter 3

Methodology

3.1 Model of a PV module

Normally, the mathematical model indicative of the dynamic variables governing the behaviour of an actual solar cell sheds more emphasis upon explaining its current and voltage (I-V) normally approximating the design of Solar Cell parameters (SC) [16, 32, 79].

These parameters critically affect the performance of the solar cells or photovoltaic (PV) modules. There are three major types of PV modules known by the number of diodes they contain. They are the Single-Diode (SD) model, the Double-Diode (DD) model, and a Triple-Diode (TD) model [7, 2, 51]. The parameters, moreover, are useful to model the inherent non-linearities of the solar cell coupled with properties like photo-generated current, diode saturation current, series resistance and diode ideality factor. In essence, accurate estimation of these parameters becomes critical in attaining an optimum trade-off between current and voltage.

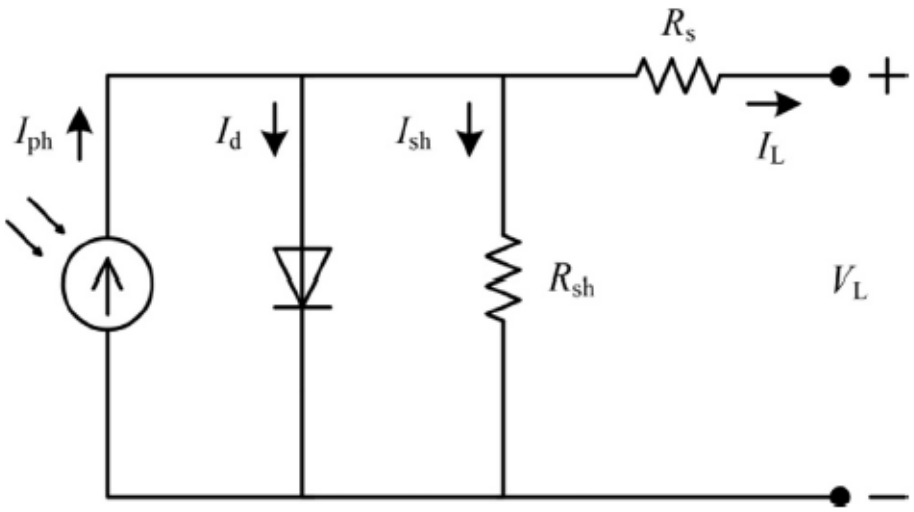

Figure 3.1: A single diode circuit model

3.1.1 Single-diode model

This is the simplest form of a PV module. It consists of a current source, one diode and two resistors [18] as shown in figure 3.1:

The output current (I_t) is given by:

$$I_t = I_{ph} - I_{sd} - I_{sh} \tag{3.1}$$

Where I_t denotes the terminal current and I_{ph}, I_{sd} and I_{sh} being the photo-generated, diode currents and shunt resistor correspondingly. In a more presentable form, making use of the Shockley diode equation we obtain:

$$I_t = I_{ph} - I_{sd}\left[\exp\left(\frac{q(V_t + R_s \cdot I_t)}{n \cdot k \cdot T}\right) - 1\right] - \frac{V_t + R_s \cdot I_t}{R_{sh}} \tag{3.2}$$

Equation (3.2) takes into account particular internal physical parameters of the diode in its model. Here, V_t represents the terminal voltage, I_{sd} represents the current of the diode saturation, while R_{sh} and R_s defines the shunt and series resistance, respectively. n is the ideality factor of the diode. Some physical constants are included because of the Shockley diode equation. They include the Boltzmann constant $k = 1.380 \times 10^{-23}(J/K)$, the charge

Table 3.1: Parameter domain range of single diode models

Parameter	**Domain range**
$R_s(\Omega)$	(0, 0.5)
$R_{sh}(\Omega)$	(0, 100)
I_{ph} (A)	(0, 1)
I_{sd} (μA)	(0, 1)
n	(1, 2)

magnitude of an electron $q = 1.602 \times 10^{-19} C$, and the temperature of the p-n junction of the cell (T). To accurately model the SD system, it is imperative to find the values of parameters R_{sh}, R_s, I_{ph}, I_{sd}, I_{sh}, and n that correspond to the measurable values of V_t and I_t.

Table 3.1 describes the ranges of parameters used in previous related studies [26] and are in turn, used in this thesis. These ranges are noted to not be randomly selected but are based on physical meaning to represent a feasible and realistic search space such that impractical solutions are not considered by any algorithm or solution method being employed [74, 56, 72, 44].

While the SD model is generally considered to be a good model for the SC, the literature shows that its accuracy is not sufficiently practical [76, 89, 80]. For this reason, the Double diode model is proposed.

3.1.2 Double-diode model

The Double Diode (DD) model is an integral of two diodes for different purposes - the first one is the rectifier of alternating current (AC) into direct current (DC), and the second one models recombination current loss and other semiconductor device imperfections and is called SC. That is to say that from these models, the dual-diode modification was implemented in the model described by Elias et al., and hence more accurate models have been developed taking into consideration non-ideal behaviours for low irradiation conditions for more precision in SC simulations and analysis [34, 38].

Figure 3.2 below shows the Double Diode (DD) arrangement depicting how two diodes can be used to recharge or control with accuracy its photo-generated current source. In this case, the arrangement is an indication of a proper design where the diodes are arranged in a row that allows for efficacy management of the current generated by the photosensitive source in the indicated arrangement.

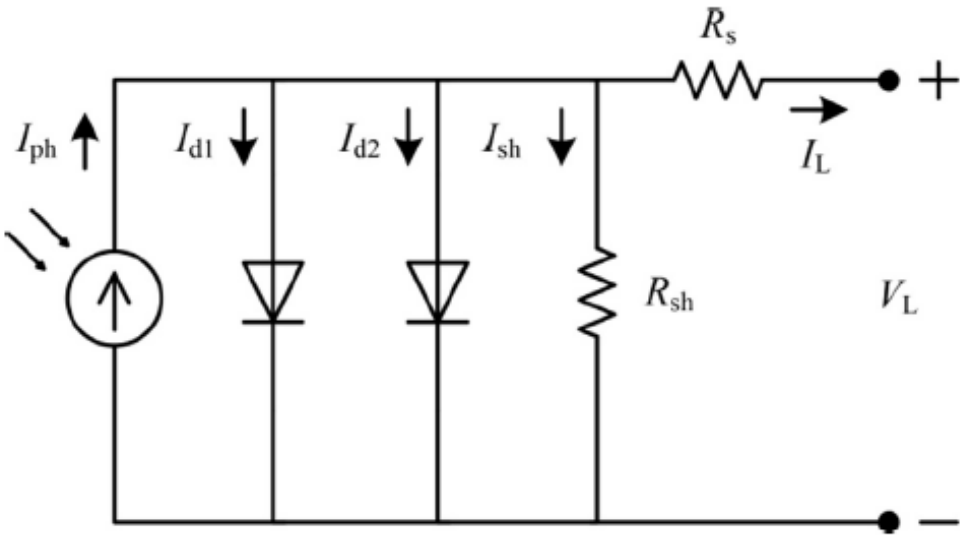

Figure 3.2: A double diode circuit model

The recombination current in microdevices represents non-ideal features from a procedure where electron-hole pairs can radiate energy while they conjugate [81]. Indeed, accurate analysis and design of SC require due consideration of several non-idealities that include recombination current, leakage current, and parasitic capacitances [95]. The DD model takes into account the dual diode configuration to be more realistic in its representation and thus it contributes to greater accuracy in simulations and analysis having these non-ideal behaviours [86].

Leveraging the figure above, (3.1) can be formulated as the following:

$$I_t = I_{ph} - I_{d1} - I_{d2} - I_{sh} \tag{3.3}$$

Where I_{d1} is the current flowing through the first diode and I_{d2} is the current flowing through the second diode. The remaining elements are specified in

(3.1). To gain insight into the internal structure of diodes, the Shockley diode equivalence [74] is employed. Subsequently, Equation (3.3) transforms, resulting in the form presented in Equation (3.4).

$$I = I_{ph} - I_{sd1}\left[\exp\left(\frac{q(V_t + Rs \cdot I_t)}{n_1 \cdot k \cdot T}\right) - 1\right] - I_{sd2}\left[\exp\left(\frac{q(V_t + Rs \cdot I_t)}{n_2 \cdot k \cdot T}\right) - 1\right] - \frac{V_t + R_s \cdot I_t}{R_{sh}} \tag{3.4}$$

Here, I_{sd2} and I_{sd1} represent the saturation and diffusion currents for diode two ($d2$) and diode one ($d1$), respectively. Additionally, $n2$ and $n1$ characterize the ideality factors for the recombination and diffusion diodes, respectively. With these considerations, the DD model entails estimating seven unknown parameters: R_s, R_{sh}, I_{ph}, I_{sd1}, I_{sd2}, $n1$, and $n2$.

3.1.3 Triple-diode model

The most recent triple-diode model is described as an upgrade of the SD and DD models. It is noted for its ability to explain better and define the different current components of large-size crystalline silicon solar cells [52, 69]. It has also been shown to address issues related to recombination currents and enhance the overall performance and reliability of the system [27, 92]. The TD model is illustrated in figure 3.3:

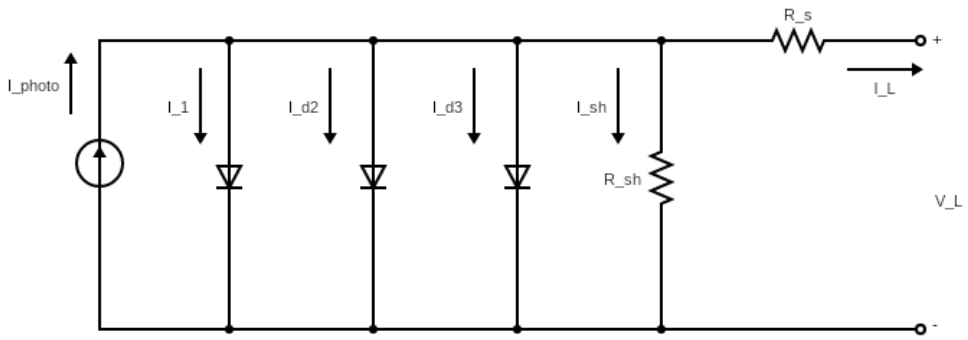

Figure 3.3: A triple diode circuit model

With the addition of an extra diode, Equation (3.3) is then modified as:

$$I_t = I_{ph} - I_{d1} - I_{d2} - I_{d3} - I_{sh} \tag{3.5}$$

Applying the Shockley equivalence, Equation (3.5) becomes

$$\begin{aligned} I = I_{ph} - I_{sd1}\left[\exp\left(\frac{q(V_t + R_s \cdot I_t)}{n_1 \cdot k \cdot T}\right) - 1\right] - I_{sd2}\left[\exp\left(\frac{q(V_t + R_s \cdot I_t)}{n_2 \cdot k \cdot T}\right) - 1\right] \ldots \\ \ldots - I_{sd3}\left[\exp\left(\frac{q(V_t + R_s \cdot I_t)}{n_3 \cdot k \cdot T}\right) - 1\right] - \frac{V_t + R_s \cdot I_t}{R_{sh}} \end{aligned} \tag{3.6}$$

The nine parameters (R_s, R_{sh}, I_{ph}, I_{sd1}, I_{sd2}, I_{sd3}, n_1, n_2 and n_3) described by the TD model are estimated to describe the relationship between current and voltage in the SC.

3.1.4 Parameter variation

Some of the aforementioned and described parameters depend on the temperature of the solar cell along with its irradiance levels. These factors have been considered by Sera et al. and De Soto et al. and are described as:

$$I_{ph} = \left(I_{pvn} k_i \Delta T\right)\frac{G}{G_n} \tag{3.7}$$

$$I_s d = I_{on}\left(\frac{T}{T_n}\right)^3 \exp\left[\left(\frac{q \cdot Eg}{\alpha \cdot k}\right)\left(\frac{1}{T_n} - \frac{1}{T}\right)\right] \tag{3.8}$$

$$E_g = E_{gn}(1 - 0.0002677\Delta T) \tag{3.9}$$

$$R_p = R_{pn}\frac{G}{G_n} \tag{3.10}$$

Where I_{ph}, I_{sd}, E_{gn}, G_n, R_{pn}, and T_n represent the photocurrent, diode reverse saturation current, material band gap, solar irradiance, shunt resistance, and cell temperature under the nominal conditions (standard test conditions, STCs), respectively [27]. E_{gn} takes a value of 1.121 eV for silicon cells [42], ΔT is the difference between T and T_n, and K_i is the coefficient of short-circuit current.

These relations are adopted to illustrate the I–V interactions of a single- and multiple-diode PV model of a PV module under various temperature and solar irradiance conditions.

3.2 Whale Optimization Algorithm

Humpback whales use a unique diving method to great depths, surrounding their targets in such a way that they build a spiral-shaped bubble net, then rise again during this process. They feed usually on small fish found near the surface of water bodies. This mathematical model of the hunting strategy tries to describe steps performed in the hunting i.e. how whales go around their prey, carry out the spiral bubble net manoeuvre and search for their intended target. This model can be analyzed and modelled as described below:

Whales extensively use a special technique to catch prey. After spotting a school of fish, they form a spiral net around their prey using bubbles to trap and drive them to the centre before swimming up to strike where the prey would be densely congregated. Scientists have been able to use mathematics to model this sequence of behaviour into an algorithm and transfer its solution protocol to different fields of science such as optimization.

3.2.1 Surrounding the prey

In the application of the WOA, the prey position is the optimal solution for the entire manoeuvre. This is logically coherent as whales would opt for the position which maximises the amount of fish they can consume with one strike. The encircling dance of the whales around the prey can be represented as such [64]:

$$D = |C \cdot X_p(t) - X(t)| \tag{3.11}$$

$$X(t+1) = X_p(t) - A.D \tag{3.12}$$

where $X(t)$ is the position vector of whale position, t denotes the current iteration, $X_p(t)$ is the prey position vector, and A and C are coefficient vectors that can be computed as:

$$A = 2a \cdot r - a \tag{3.13}$$

$$a = 2 - 2 \cdot \left(\frac{t}{\text{iterations}_{\max}} \right) \tag{3.14}$$

$$C = 2 \cdot r \tag{3.15}$$

The vector a is linearly decreasing from two to zero with each step length depending on the ratio of the step count to the maximum number of iterations. While $r \in \text{rand}(0, 1)$ and changes with each iterative step.

3.2.2 Attacking the prey

This process includes the random combination of two states which are ultimately selected via the randomness of the variables of each iteration. In one case where $|A| < 1$ from equation (3.13), the whales or solution points employ equation (3.12) to close in on the prey (optimal solution). In another case where $|A| > 1$, the whales use a spiral behaviour to further explore the solution space. This can be computed as [64]:

$$X(t+1) = D' \cdot e^{bl} \cos(2\pi l) + X_p(t) \tag{3.16}$$

$$D' = |X_p(t) - X(t)| \tag{3.17}$$

Where b is a constant that informs the shape of the log component of the periodic function, and l is such that $l \in \text{rand}[-1, 1]$.

The solution points simultaneously leverage this surround-and-attack protocol with each iteration with an equal chance. This creates a contracting spiral path that closely resembles the behaviour of whales while hunting. The combined behaviour can be modelled as such:

$$X(t+1) = \begin{cases} X_p(t) - A \cdot D & \text{if } p < 0.5 \\ D' \cdot e^{bl} \cdot \cos(2\pi l) + X_p(t) & \text{if } p \geq 0.5 \end{cases} \tag{3.18}$$

3.2.3 Hunting the Prey

In reality, not all whales involved in the search may communicate effectively with the whale closest to the prey and may wander and search randomly of their own volition to find food. This necessitates the use of a coefficient A that will depict the likelihood that an individual whale follows the whale closest to the prey or attempts an individual search for the next iterative time frame. This behaviour is modelled as follows [64]:

$$D = |C \cdot X_r(t) - X(t)| \tag{3.19}$$

$$X(t+1) = X_r(t) - A \cdot D \tag{3.20}$$

where r is a random search agent.

The flowchart of the WOA is illustrated in Fig 3.4

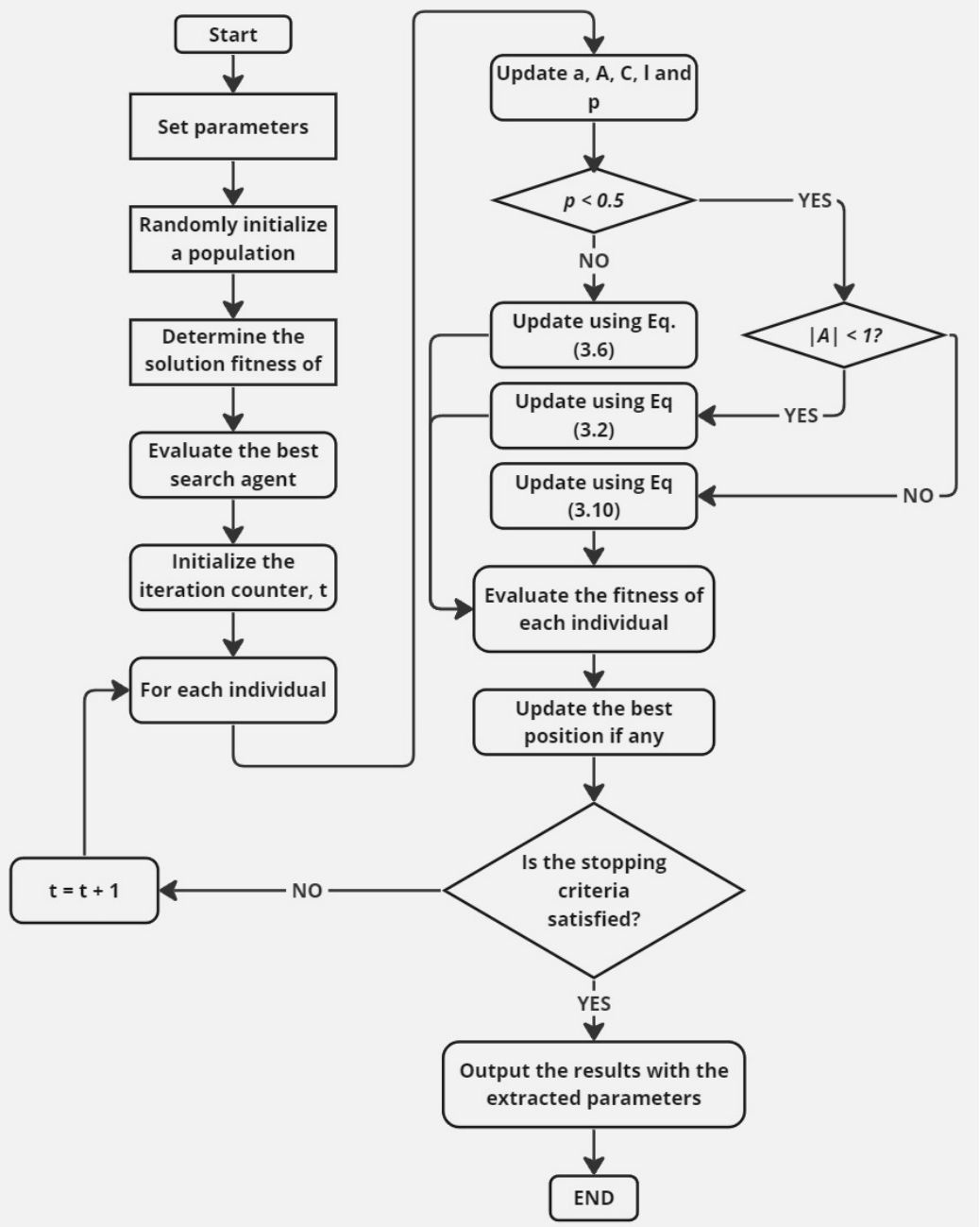

Figure 3.4: The WOA flowchart

3.3 Improved Whale Optimization Algorithm

In a paper written by Xiong et al., an improved form of the WOA (IWOA) was posited in the context of photovoltaic parameter estimation. This was because the base form of the WOA tended to get trapped in local optima due to its quick convergence at the commencement of the evolutionary phase as shown by the behaviour of the coefficient $|A|$. While this is not a problem when considering unimodal problems, it poses a problem with facing multimodal problems of which the estimation of triple diode PV systems are.

It was shown that since the coefficient $|A|$ serves to oscillate the algorithm between exploration and exploitation, the likelihood of these cases per iteration is not the same [100]. Equation (3.13) can be written as:

$$\begin{aligned} A &= 2a \cdot \text{rand}(0,1) - a \\ &= \left[2 \cdot \text{rand}(0,1) - 1\right] \cdot a \\ &= \gamma \cdot a \end{aligned} \tag{3.21}$$

where $\gamma = 2 \cdot \text{ rand } (0,1) - 1$, and is a real number which is uniformly distributed such that $\gamma \in (-1,1)$. Now since a is linear and reducing from 2 to 0 over t iterations, it holds that $|A| = |\gamma \cdot a| < 1$ for the last half of the iterative processes as shown in fig 3.5.

Xiong et al. also showed that the probability of the WOA executing (3.12) can be expressed as:

$$\begin{aligned} P(|A| < 1) = P(|\gamma \cdot a| < 1) &= 0.5 + \int_{0.5}^{1} \int_{1}^{\frac{1}{\gamma}} \mathrm{d}a \cdot \mathrm{d}\gamma \\ &= 0.5 + \int_{0.5}^{1} \left(\frac{1}{\gamma} - 1\right) d\gamma \\ &= 0.5 + (\ln \gamma - \gamma)\Big|_{0.5}^{1} \\ &= \ln 2 \approx 0.693 \end{aligned} \tag{3.22}$$

This shows that in the first half of the iterative process, the whales display about a 0.7 probability of exhibiting exploratory behaviour by adjusting their direction of search based on another random search agent (who is not

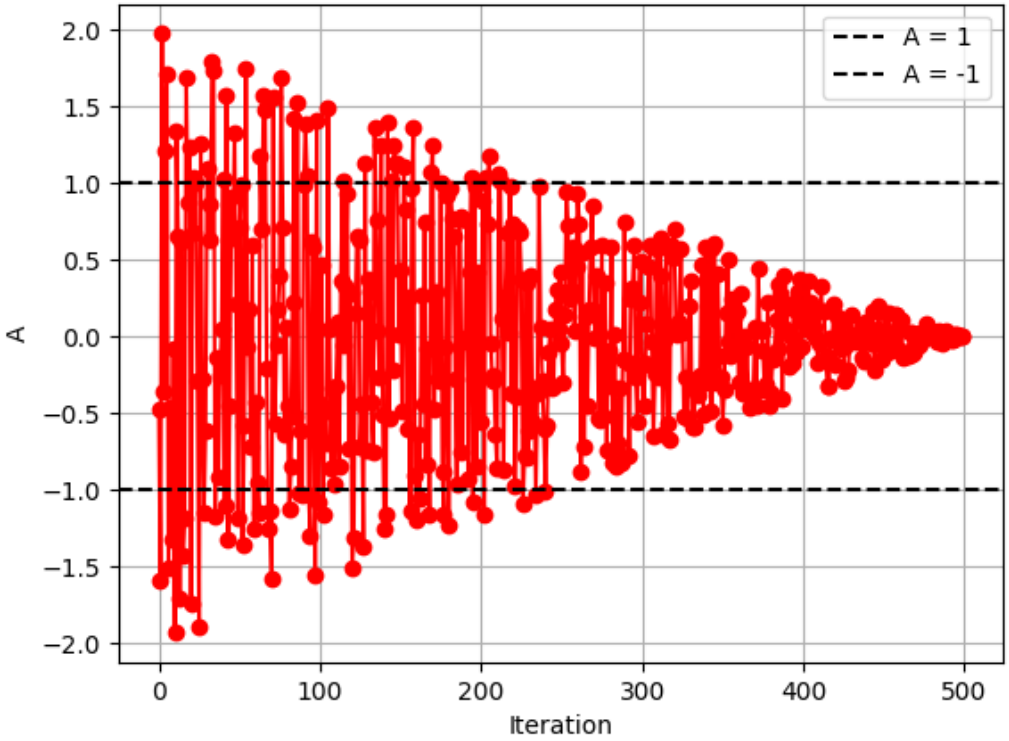

Figure 3.5: Distribution of A for linearly decreasing values of a

the closest to the prey). Including the additional probability of the search agents following a spiral path, it was shown by Xiong et al.that exploration heavily dominates the algorithm for the first half of the process. But this quickly shrinks during the second half which leaves the algorithm vulnerable to getting trapped in local minima as illustrated in figure 3.5. To balance exploration and exploitation, Xiong et al. proposed two additional search strategies to replace equations 3.20 and 3.12 respectively:

$$X(t+1) = X_{r_1}(t) - A \cdot |X(t) - X_{r_1}(t)| \tag{3.23}$$

$$X(t+1) = X_{r_1} - A \cdot |X_p(t) - X_{r_2}(t)| \tag{3.24}$$

where r_1 and r_2 are random search agents. Xiong et al. claimed through sufficient evidence that the use of random agents increases the diversity of the population and improves the exploration capabilities in a more balanced manner. Furthermore, the exclusion of the coefficient C reduces some randomness in the search processes but this apparent reduction in randomness is replaced by the new search strategy which guarantees a more consistently robust search. The flowchart of Xiong et al.'s improved algorithm is illustrated in figure 3.6.

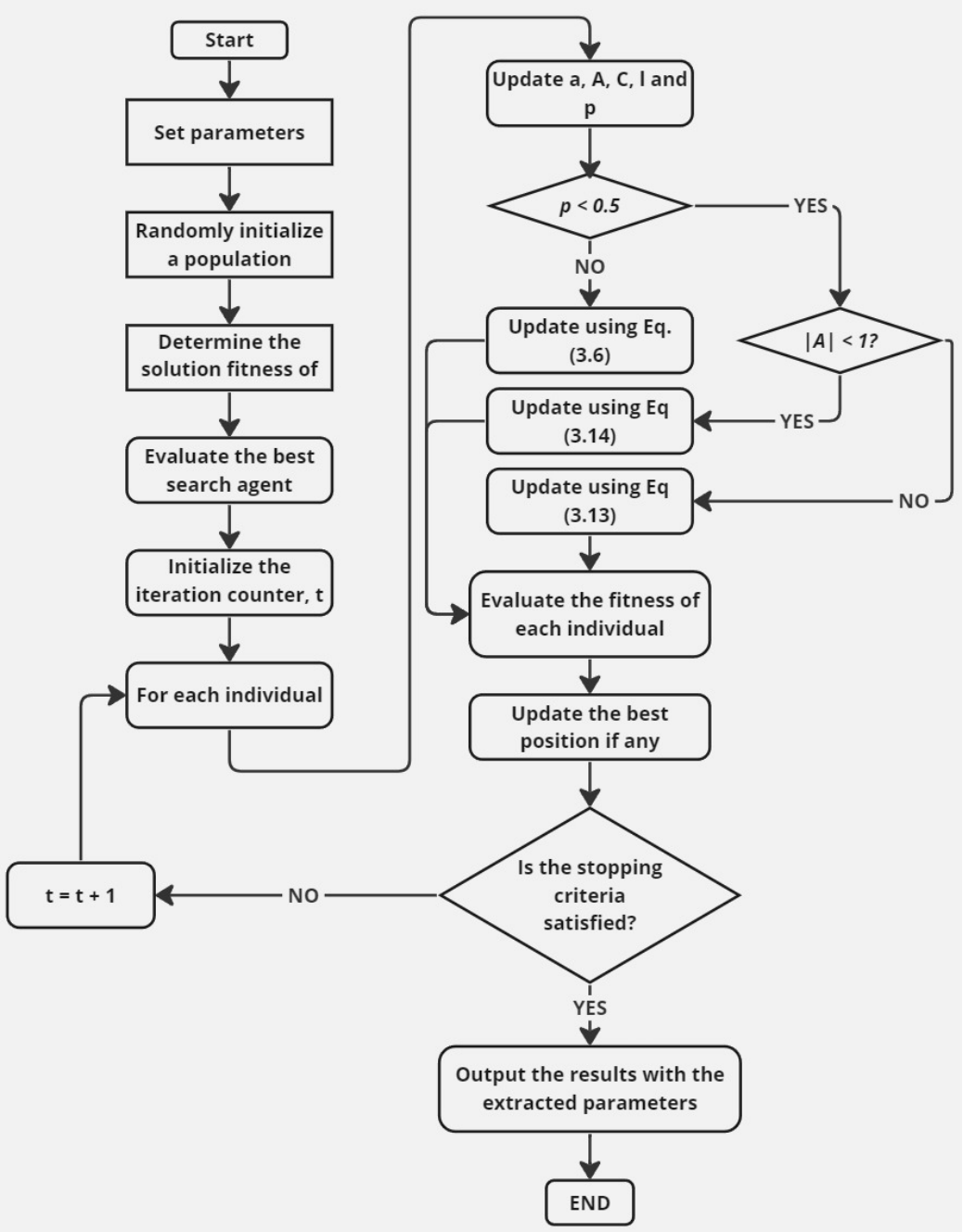

Figure 3.6: The IWOA flowchart

3.4 Modification Evaluation Criteria

This section covers the methodology adopted to evaluate and assess the modifications made to the Improved Whale Optimization Algorithm, in the context of tuning the exploitation and exploratory capabilities/likelihood of the algorithm. The types of tests adopted are outlined and the rationale explained.

To evaluate the efficacy of the proposed modifications, ten benchmark functions were adopted in this thesis. Six were unimodal (having one solution) and four were multimodal (having multiple solutions). The benchmark functions used in this thesis are shown in table 3.2

Name	**Formula**	**Global Minimum**	**Search Domain**
Sphere Function [68]	$f_1(\mathbf{x}) = \sum_{i=1}^{n} x_i^2$	0 at $\mathbf{x} = 0$	$-100 \leq x_i \leq 100$
Sum of Absolute Values [31]	$f_2(\mathbf{x}) = \sum_{i=1}^{n} \lvert x_i \rvert + \prod_{i=1}^{n} \lvert x_i \rvert$	0 at $\mathbf{x} = 0$	$-10 \leq x_i \leq 10$
Sum of Squares Function [68]	$f_3(\mathbf{x}) = \sum_{i=1}^{n} \left(\sum_{j=1}^{i} x_j \right)^2$	0 at $\mathbf{x} = 0$	$-10 \leq x_i \leq 10$
Rosenbrock Function [23, 68]	$f_5(\mathbf{x}) = \sum_{i=1}^{n-1} [100(x_{i+1} - x_i^2)^2 + (x_i - 1)^2]$	0 at $\mathbf{x} = 1$	$-2.048 \leq x_i \leq 2.048$
Step Function [21]	$f_6(\mathbf{x}) = \sum_{i=1}^{n} (x_i + 0.5)^2$	0 at $\mathbf{x} = -0.5$	$-100 \leq x_i \leq 100$
Quartic Function [21]	$f_7(\mathbf{x}) = \sum_{i=1}^{n} i \cdot x_i^4 + \text{random}[0, 1]$	0 at $\mathbf{x} = 0$	$-1.28 \leq x_i \leq 1.28$
Schwefel Function [68]	$f_8(\mathbf{x}) = \sum_{i=1}^{n} -x_i \sin(\sqrt{\lvert x_i \rvert})$	$418.9829n$ at $\mathbf{x} = 420.9687$	$-500 \leq x_i \leq 500$
Rastrigin Function [83, 68]	$f_9(\mathbf{x}) = \sum_{i=1}^{n} [x_i^2 - 10\cos(2\pi x_i) + 10]$	0 at $\mathbf{x} = 0$	$-5.12 \leq x_i \leq 5.12$
Ackley Function [8, 68, 103]	$f_{10}(\mathbf{x}) = -20 \exp\left(-0.2\sqrt{\frac{1}{n}\sum_{i=1}^{n} x_i^2}\right)$ $- \exp\left(\frac{1}{n}\sum_{i=1}^{n} \cos(2\pi x_i)\right) + 20 + e$	0 at $\mathbf{x} = 0$	$-32 \leq x_i \leq 32$
Griewank Function [68]	$f_{11}(\mathbf{x}) = \frac{1}{4000}\sum_{i=1}^{n} x_i^2 - \prod_{i=1}^{n} \cos\left(\frac{x_i}{\sqrt{i}}\right) + 1$	0 at $\mathbf{x} = 0$	$-600 \leq x_i \leq 600$

Table 3.2: Benchmark Functions

To highlight the performance of the modifications from a statistical perspective, the mean and standard deviation of the last ten fitness values will be computed for each benchmark function and tabulated for clarity.

3.5 Exploratory Modifications

This section explores the methodology used to modify the IWOA to boost its exploratory capabilities and robustness. The modifications were tested using 10 benchmark functions, 6 of which were unimodal (having one optimum) while the remaining 4 were multi-modal with many local optima but one global optimum. The performance of the variations was illustrated by plotting the number of iterations and the fitness value for 10 distinct experiments, for each benchmark function. Furthermore, a statistical overview was done to comprehensively analyse the means and standard deviation of the last fitness values of the 10 experiments for each benchmark function. The best-performing exploratory modification will be selected and applied to the research case of estimating the parameters of the triple-diode PV system.

As highlighted, the value of $|A|$ serves as a metric that leads the algorithm to either exploration or exploitation after the value of p has been randomized for the current iterative step. This infers that the manipulation of the properties of the component variable 'a' can in turn adjust the distribution spread or likelihood of $|A|$ values which fall below or above 1.

To improve the robustness and exploratory capability of the IWOA even further, the following functions in the next few subsections were considered in replacement of equation (3.14).

These modifications to the IWOA were tested using unimodal and multimodal benchmark functions [68] as shown in table 3.3 to 3.6. Experiments were performed and graphed for each modification, across the 10 different benchmark functions. All benchmark tests and experiments were carried out on a 3.3-GHz AMD Ryzen 5 5600H Radeon processor (12 CPUs) with 16.0 GB RAM using Python 3.11.2.

3.5.1 Sinusoidal variation

This variation of a adopts the sine function to introduce periodicity in the randomly converging spread of the values of A.

$$a = 2 + \sin\left(\frac{2\pi i}{\max_{\text{iter}}}\right) \tag{3.25}$$

Where i is the ith iteration in the range of maximum epochs. This variation ensures that the algorithm maintains a more exploratory stance even after the first half of the total iterations as shown in figure 3.7. For the sample experiment displayed, of the 500 epochs, a total of 225 iterations of $|A|$ lay above 1 while the remaining 275 were below which is a more balanced distribution compared with the classic case. The function allows for some exploratory behaviour towards the end of the search. This gives room for the algorithm to be more likely to escape possible local minima.

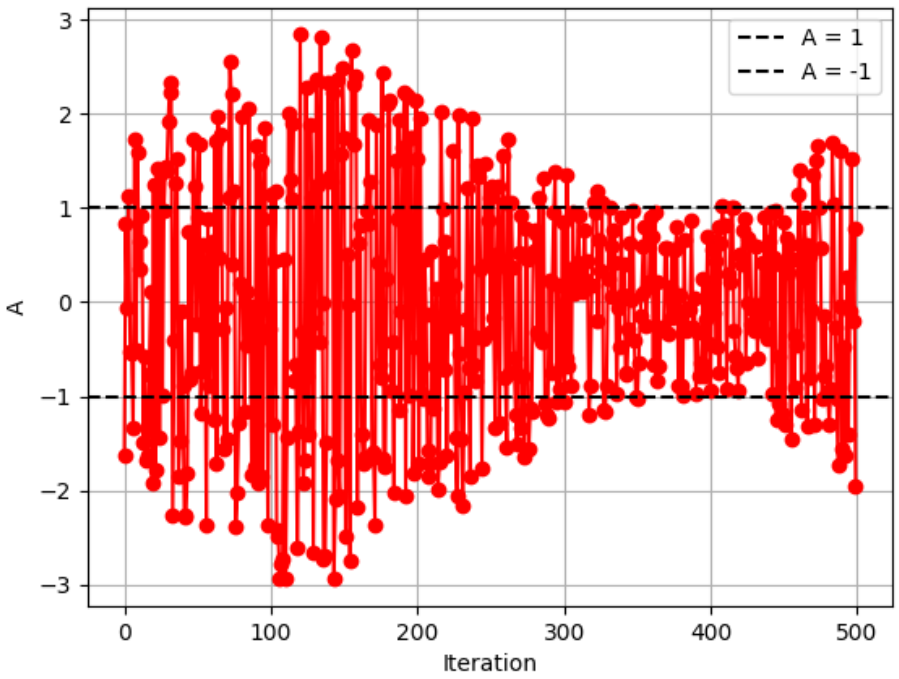

Figure 3.7: The distribution of A for the sinusoidal variation of a

Benchmark tests were carried out on the IWOA after the sinusoidal variation of a was adopted in the algorithm. Convergence was rather quick for the unimodal functions apart from the quartic function in figure 3.8f due to noise. Regardless of the unimodality of the other functions, a few delays in convergence were detected as a result of the increased exploratory predisposition of the modified algorithm. This means that in the unimodal case where there exists just one solution, the algorithm will still prefer to "look around" just to make sure. And this extra space search causes some delays in convergence speed. While not generally ideal, for the thesis objective of increased robustness, this serves our eventual needs.

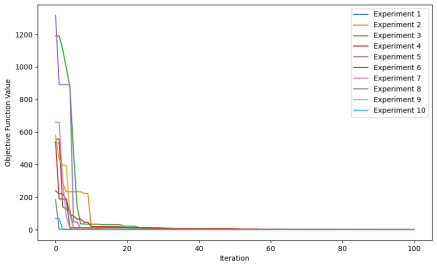

(a) Sphere function

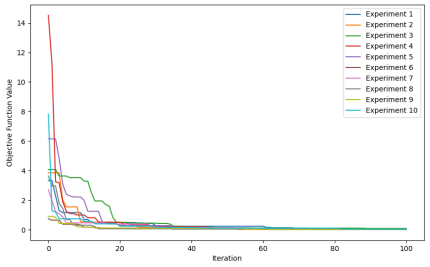

(b) Sum of absolutes

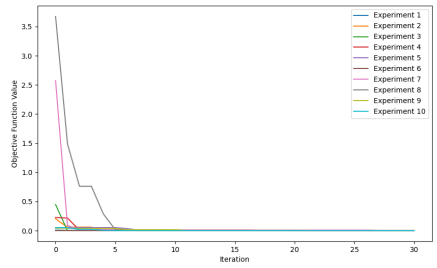

(c) Sum of squares

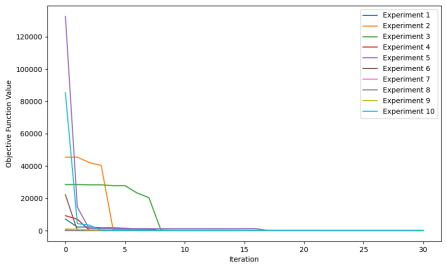

(d) Rosenbrock function

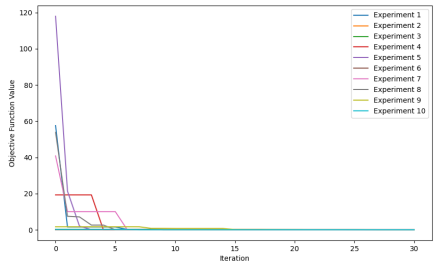

(e) Step function

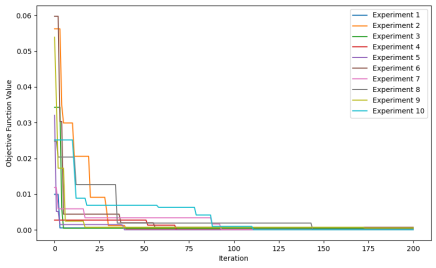

(f) Quartic function (with noise)

Figure 3.8: Performance of the sinusoidal variation on uni-modal benchmark functions

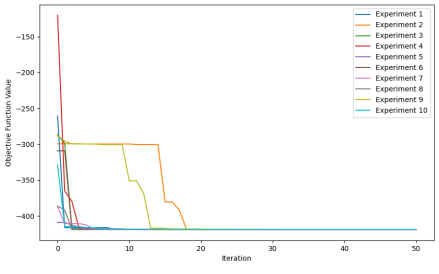

(a) Schwefel function

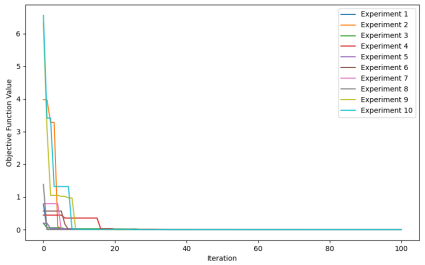

(b) Rastrigin function

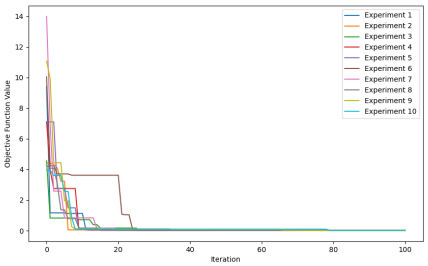

(c) Ackley function

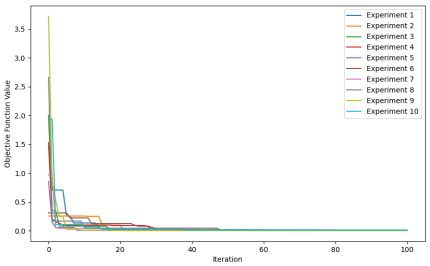

(d) Griewank function

Figure 3.9: Performance of the sinusoidal variation on multi-modal benchmark functions

As for the multimodal functions, the modifications assisted the algorithm to escape the local minima in two separate experiments in the Schwefel function as shown in figure 3.9a, after less than 18 iterations. This will take longer in a case where the IWOA did not have a sufficiently higher exploratory likelihood. One experiment was observed to plateau for a little under 20 iterations before escaping the local minimum and converging to the global optimum like the rest as shown in figure 3.9c.

Table 3.3: Statistical overview for the sinusoidal variation's performance on benchmark functions

Function	**Domain range**	**Global Minimum**	**Epochs**	**Dimension**	**Mean of last fitness**	**Std. dev. of last fitness**
Sphere	(-100, 100)	0	500	2	1.0547×10^{-3}	1.4372×10^{-3}
Sum of absolute values	(-10,10)	0	500	2	1.1345×10^{-3}	1.0334×10^{-3}
Sum of squares	(-10, 10)	0	500	2	6.08×10^{-10}	7.05×10^{-10}
Rosenbrock	(-2.048, -2.048)	0	500	2	1.15398×10^{-4}	2.6038×10^{-4}
Step	(-100, 100)	0	500	2	2.7083×10^{-4}	3.1478×10^{-4}
Quartic (with noise)	(-1.28,1.28)	0	500	9	5.54498×10^{-2}	3.8289×10^{-2}
Schwefel	(-500, 500)	418.9829	500	1	4.189829×10^{2}	3.99×10^{-6}
Rastrigin	(-5.12, 5.12)	0	500	2	2.7568×10^{-1}	4.2866×10^{-1}
Ackley	(-32, 32)	0	500	2	1.5969×10^{-2}	8.6136×10^{-3}
Griewank	(-600, 600)	0	500	2	4.1652×10^{-2}	3.4596×10^{-2}

A statistical analysis was executed on the last fitness of each experiment to ascertain the average performance of the modification, as well as the standard deviation of these last fitness values, across all benchmark tests. The table 3.3 shows the results, including all the necessary details to make the modification performance more comprehensive. The variation allowed the modified IWOA to perform quite well against all but the Rastrigin function which had a high mean of 2.756×10^{-1} even after 500 iterations.

3.5.2 Oscillatory variation

A periodic function can be used to either increase or decrease the distribution likelihood of points of A which lie above or below 1 for every iteration. The equation for this variation is given by:

$$a = 1.5 + \sin\left(i \cdot \frac{\pi}{\max_{\text{iter}}}\right) \tag{3.26}$$

In such cases, we define all possible behaviours to be distributed across half the cycle of a sine function as $\frac{i}{\max_{\text{iter}}}$ approaches 1 for any maximum number of iterations. The behaviour for a random experiment is shown in figure 3.10

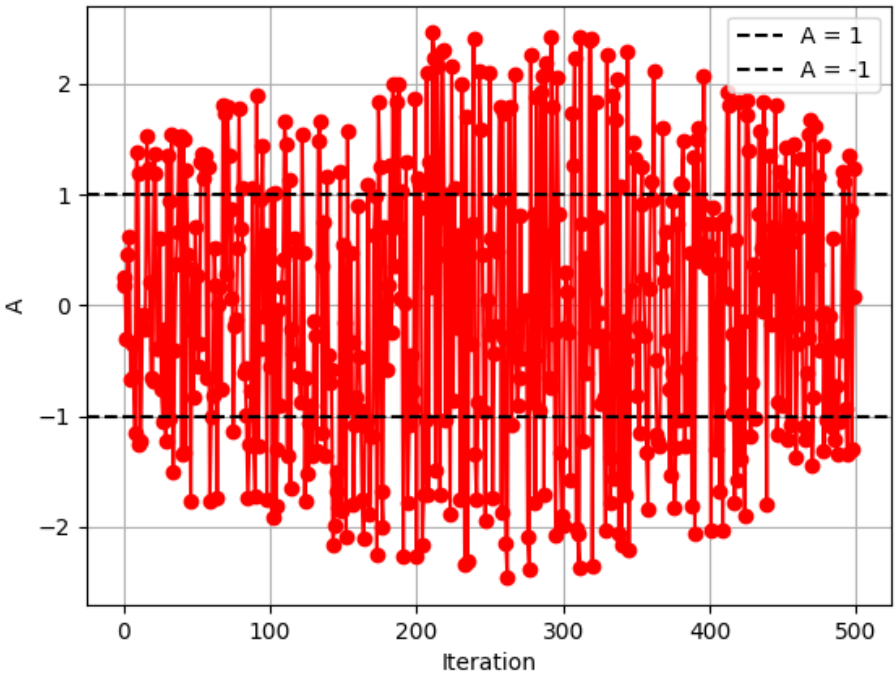

Figure 3.10: The distribution of A for the oscillatory variation of a

For a typical random experiment with 500 iterations, 265 points lay outside the $A(-1, 1)$ interval, while the remaining 235 lay within. Compared to the classic linearly decreasing a, this modification ensures that $|A|$ maintains a more even spread of exploration and exploitation likelihood throughout the entire evolutionary phase.

The variation shows a quickly convergent behaviour on unimodal functions with the longest taking a little under 20 iterations to converge. Unlike the sinusoidal variation, this variation handled the quartic function quite well with only one experiment converging past 40 iterations due to noise.

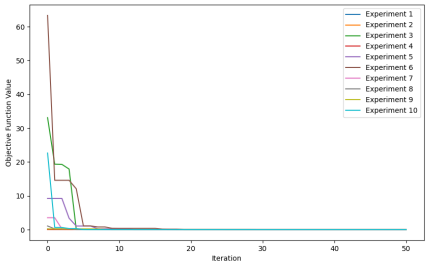

(a) Sphere function

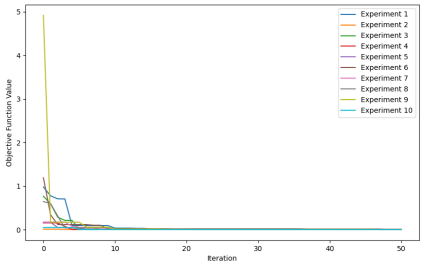

(b) Sum of absolutes

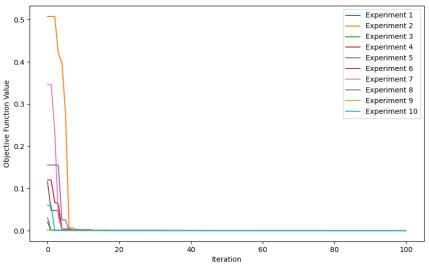

(c) Sum of squares

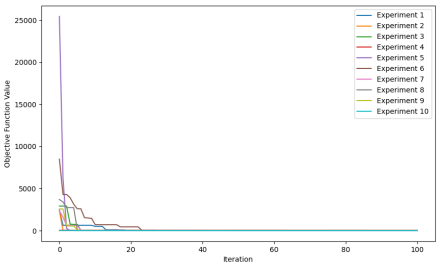

(d) Rosenbrock function

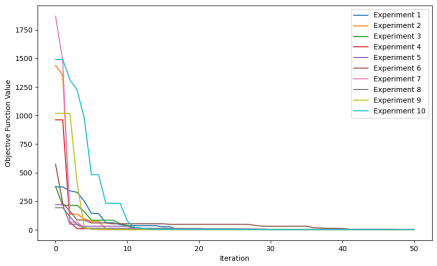

(e) Step function

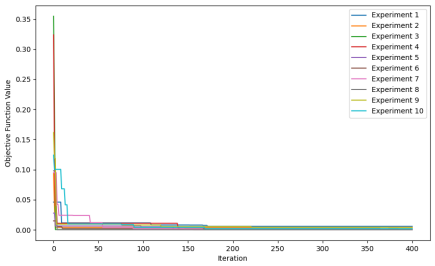

(f) Quartic function (with noise)

Figure 3.11: Performance of the oscillatory variation on uni-modal benchmark functions

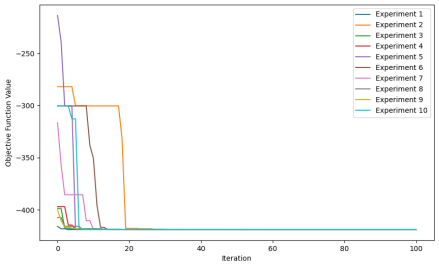

(a) Schwefel function

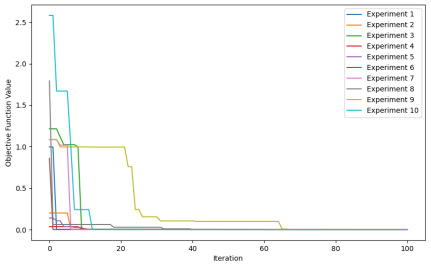

(b) Rastrigin function

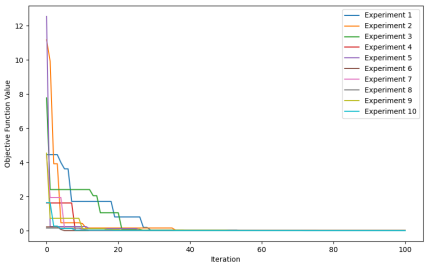

(c) Ackley function

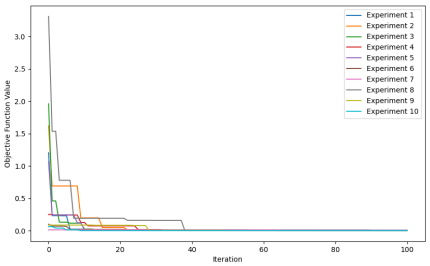

(d) Griewank function

Figure 3.12: Performance of the Oscillatory variation on multi-modal benchmark functions

Table 3.4: Statistical overview for the oscillatory variation's performance on benchmark functions

Function	**Domain range**	**Global Minimum**	**Epochs**	**Dimension**	**Mean of last fitness**	**Std. dev. of last fitness**
Sphere	(-100, 100)	0	500	2	6.4987×10^{-4}	7.3814×10^{-4}
Sum of absolute values	(-10, 10)	0	500	2	1.4544×10^{-3}	1.0189×10^{-3}
Sum of squares	(-10, 10)	0	500	2	1.53×10^{-9}	1.47×10^{-9}
Rosenbrock	(-2.048, 2.048)	0	500	2	2.1202×10^{-4}	5.0749×10^{-4}
Step	(-100, 100)	0	500	2	2.6646×10^{-4}	2.1807×10^{-4}
Quartic (with noise)	(-1.28, 1.28)	0	500	9	7.8877×10^{-2}	7.8642×10^{-2}
Schwefel	(-500, 500)	418.9829	500	1	4.1898×10^{2}	7.20×10^{-7}
Rastrigin	(-5.12, 5.12)	0	500	2	1.4185×10^{-2}	2.8252×10^{-2}
Ackley	(-32, 32)	0	500	2	2.6838×10^{-2}	1.6937×10^{-2}
Griewank	(-600, 600)	0	500	2	4.0244×10^{-2}	4.4035×10^{-2}

The statistical overview of the performance of the oscillatory variation of the IWOA is shown in table 3.4. Across the unimodal functions, the variation performed best on the sum of squares function with a mean convergence of 1.53×10^{-9} across 10 experiments.

3.5.3 Inverse Relationship

This modification leverages an inverse function that provides a high likelihood at the beginning which slowly decreases as more iterations are carried out. By adjusting the coefficients of the function, we're able to make sure that there exist more points of A such that $A \notin (-1, 1)$ (for some point). This improves the algorithm's robustness as the search algorithm's stance becomes more exploratory above the first half of the evolutionary phase as shown in figure 3.13. The equation for this modified parameter a is given by:

$$a = 2 \cdot \left(1 + \frac{i}{\max_{\text{iter}}}\right)^{-1} \tag{3.27}$$

The modification was seen to pass the uni-modal and multi-modal functions that they were given. Convergence occurred quickly on the uni-modal functions as shown in figure 3.14, with the latest convergence occurring at the 60th iteration for the sum of absolutes functions. As shown in figure 3.14c, one of the experiments experienced a slight stagnation before escaping and converging further while being tested on the uni-modal sum of squares function.

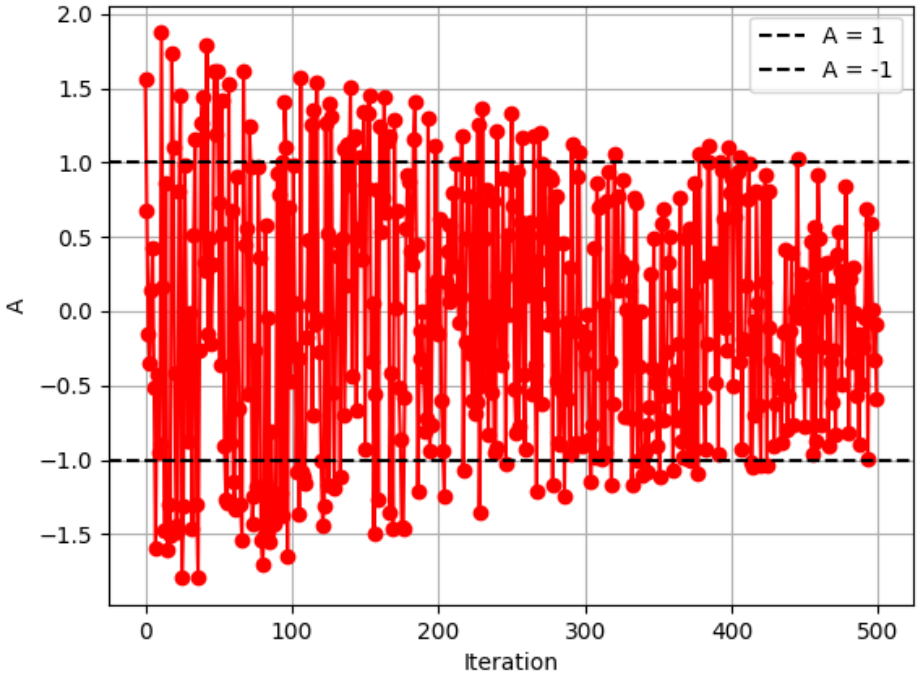

Figure 3.13: The distribution of A for the inverse variation of a

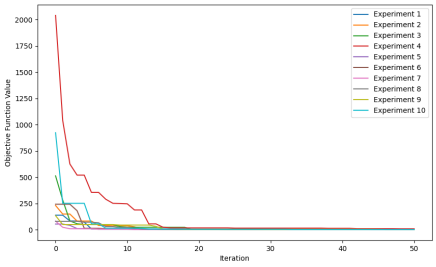

(a) Sphere function

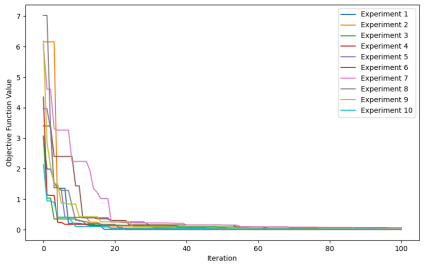

(b) Sum of absolutes

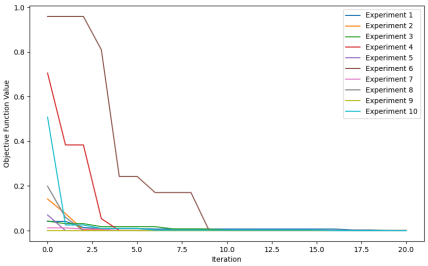

(c) Sum of squares

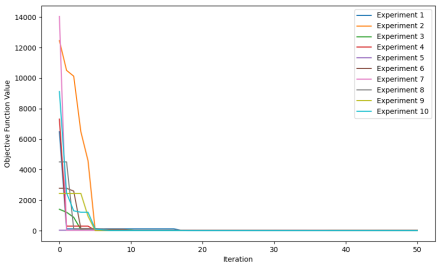

(d) Rosenbrock function

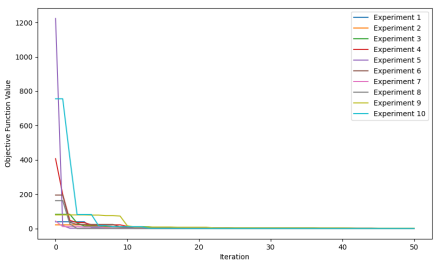

(e) Step function

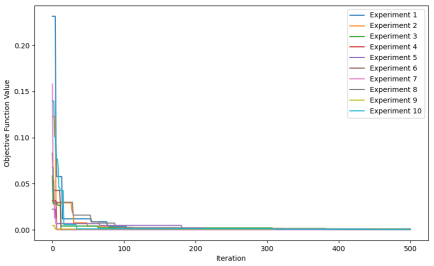

(f) Quartic function (with noise)

Figure 3.14: Performance of the inverse variation on uni-modal benchmark functions

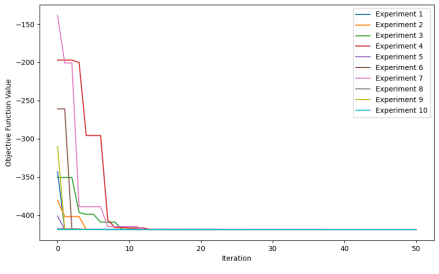

(a) Schwefel function

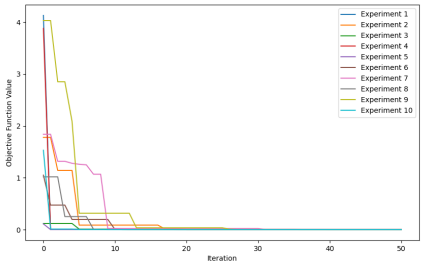

(b) Rastrigin function

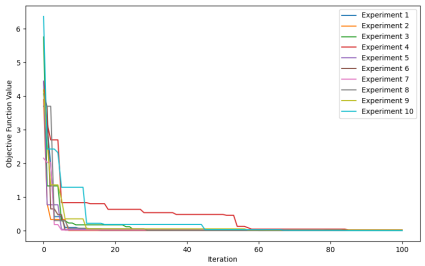

(c) Ackley function

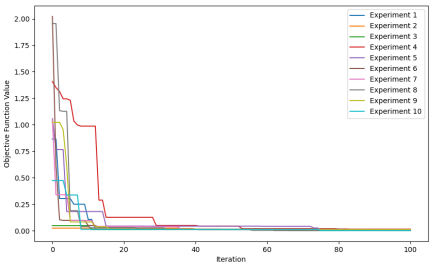

(d) Griewank function

Figure 3.15: Performance of the inverse variation on multi-modal benchmark functions

As for the multi-modal functions in figure 3.13, the modification was able to break out of local minima quite reliably, with the longest time being stuck, which was for a bit over 50 iterations for the Ackley function. With a sufficient amount of exploratory likelihood, the scheme showed a decent ability to escape local minima given an extended number of iterations. Table 3.5 shows the statistical overview of the performance of the inverse variation. The modification performed decently across the board with the weakest performance being on the Quartic and Griewank functions.

Table 3.5: Statistical overview for the inverse variation's performance on benchmark functions

Function	**Domain range**	**Global Minimum**	**Epochs**	**Dimension**	**Mean of last fitness**	**Std. dev. of last fitness**
Sphere	(-100, 100)	0	500	2	6.4420×10^{-4}	1.2359×10^{-3}
Sum of absolute values	(-10, 10)	0	500	2	1.3076×10^{-3}	1.0470×10^{-3}
Sum of squares	(-10, 10)	0	500	2	4.73×10^{-10}	4.53×10^{-10}
Rosenbrock	(-2.048, 2.048)	0	500	2	9.24×10^{-6}	1.97×10^{-5}
Step	(-100, 100)	0	500	2	2.0034×10^{-3}	3.4020×10^{-3}
Quartic (with noise)	(-1.28, 1.28)	0	500	9	6.3643×10^{-2}	3.6556×10^{-2}
Schwefel	(-500, 500)	418.9829	500	1	4.1898×10^{2}	1.42×10^{-6}
Rastrigin	(-5.12, 5.12)	0	500	2	3.2107×10^{-4}	4.9108×10^{-4}
Ackley	(-32, 32)	0	500	2	1.8405×10^{-2}	2.0925×10^{-2}
Griewank	(-600, 600)	0	500	2	4.7828×10^{-2}	4.5765×10^{-2}

3.5.4 Exponential decrease

This modification on a uses a nonlinear decrease in the form of an exponential decay to guide the spread of the output of A. Similar to the inverse modification, we attempt to have more guided control of the amount of A values below 1, per iteration. The equation for this relation is as follows:

$$a = 2.5 \cdot \exp\left(\frac{-i}{\max_{\text{iter}} - 1}\right) \tag{3.28}$$

Using the coefficient of the exponential function, we can adjust the amplitude of the distribution of A values to ensure some more exploration-guided iterations, even after the middle mark. A random experiment revealed that for 500 maximum iterations for $|A|$, a total of 162 points were above 1 while the remaining 338 lay below 1 as illustrated in figure 3.16

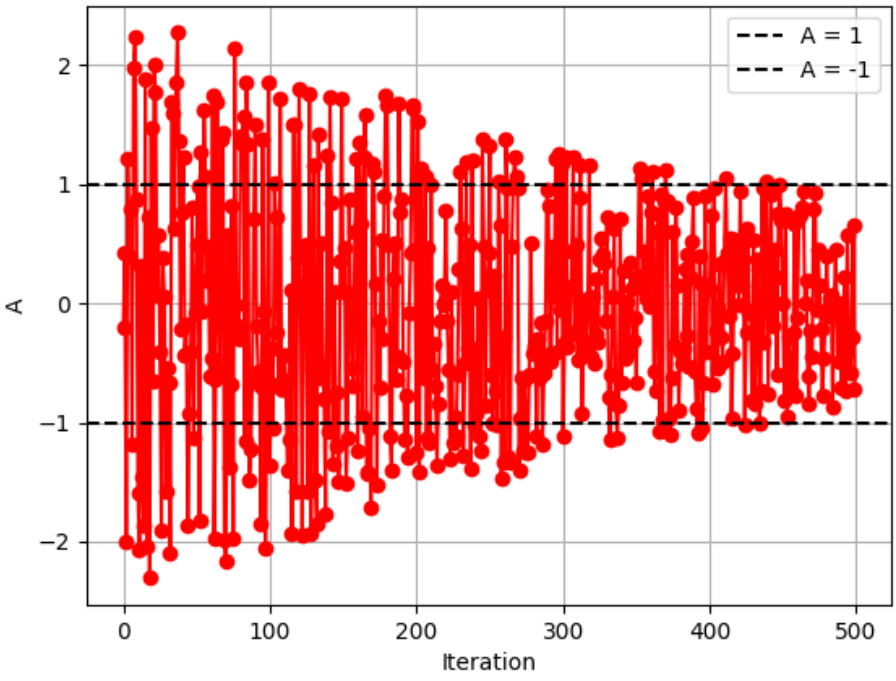

Figure 3.16: The distribution of A for the exponential decrease of a

This will imply a greater likelihood of search agents subscribing to a more exploratory stance, than the classic case. The graphical performance showed that the modification was able to converge to the global minima on the benchmark tests given to it. It was also seen in figures 3.18a and 3.18b to be able to break out of local minima. The statistical overview of the modification is shown in table 3.6

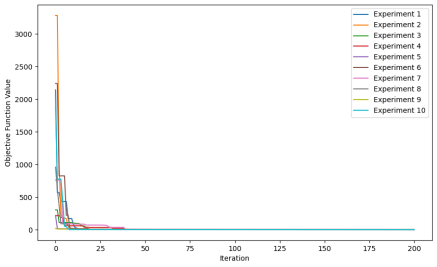

(a) Sphere function

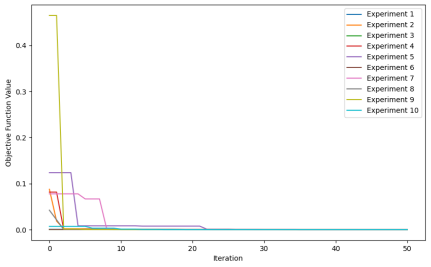

(b) Sum of absolutes

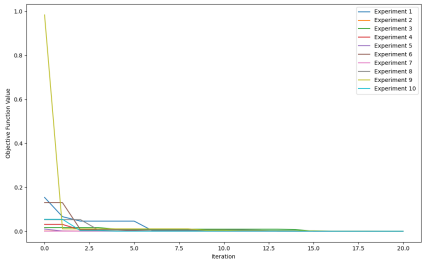

(c) Sum of squares

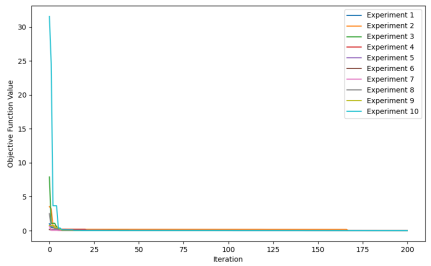

(d) Rosenbrock function

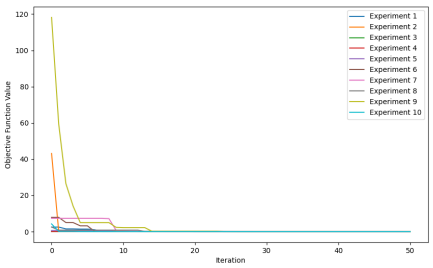

(e) Step function

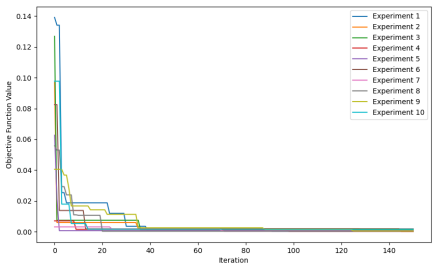

(f) Quartic function (with noise)

Figure 3.17: Performance of the exponential-decrease variation on uni-modal benchmark functions

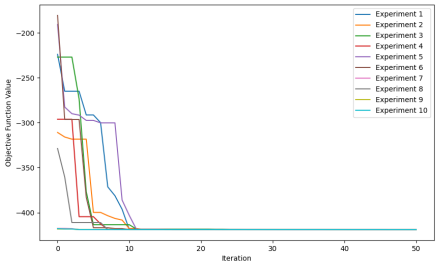

(a) Schwefel function

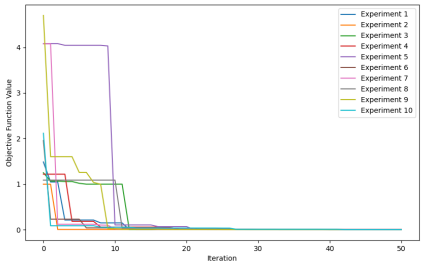

(b) Rastrigin function

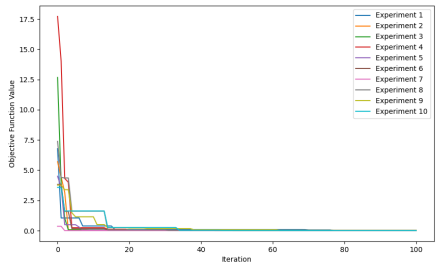

(c) Ackley function

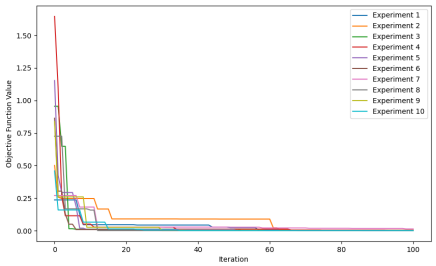

(d) Griewank function

Figure 3.18: Performance of the exponential-decrease variation on multi-modal benchmark functions

Table 3.6: Statistical overview for the exponential variation's performance on benchmark functions

Function	**Domain range**	**Global Minimum**	**Epochs**	**Dimension**	**Mean of last fitness**	**Std. dev. of last fitness**
Sphere	(-100, 100)	0	500	2	1.1836×10^{-3}	2.3092×10^{-3}
Sum of absolute values	(-10, 10)	0	500	2	2.3663×10^{-3}	3.4024×10^{-3}
Sum of squares	(-10, 10)	0	500	2	9.20×10^{-10}	1.66×10^{-9}
Rosenbrock	(-2.048, 2.048)	0	500	2	6.42×10^{-5}	1.7681×10^{-4}
Step	(-100, 100)	0	500	2	2.8941×10^{-4}	1.8834×10^{-4}
Quartic (with noise)	(-1.28, 1.28)	0	500	9	4.1799×10^{-2}	2.4264×10^{-2}
Schwefel	(-500, 500)	418.9829	500	1	4.1898×10^{2}	7.74×10^{-7}
Rastrigin	(-5.12, 5.12)	0	500	2	2.9937×10^{-1}	4.5702×10^{-1}
Ackley	(-32, 32)	0	500	2	1.5656×10^{-2}	1.0228×10^{-2}
Griewank	(-600, 600)	0	500	2	5.5895×10^{-2}	3.8900×10^{-2}

3.6 Exploitation modifications

This section explores two methodologies that can be potentially used to modify and rudder the IWOA for more exploitation in a contained manner. As in the exploratory cases above, these modifications were plotted so that their behaviour and spread of likelihood are comprehensible, and their performances were tested using the same benchmark functions above. Statistical analysis was again performed on the last fitness generated by each of the 10 experiments and the insights were recorded and shown from table 3.7 and 3.8.

3.6.1 Quadratic Decrease

This modification leverages a non-linear decreasing behaviour of a by using a special quadratic decay as shown in equation 3.29. By setting the constant to 0.14, we can ensure that out of the 500 iterations, values of $|A|$ from the 200th iteration and upwards will be strictly less than 1. This ensures an even quicker convergence to minima which may be useful in unimodal cases to reduce computation resources.

$$a = \left(\frac{14}{100} - \frac{i}{\max_{\text{iter}} - 1} \right)^2 \tag{3.29}$$

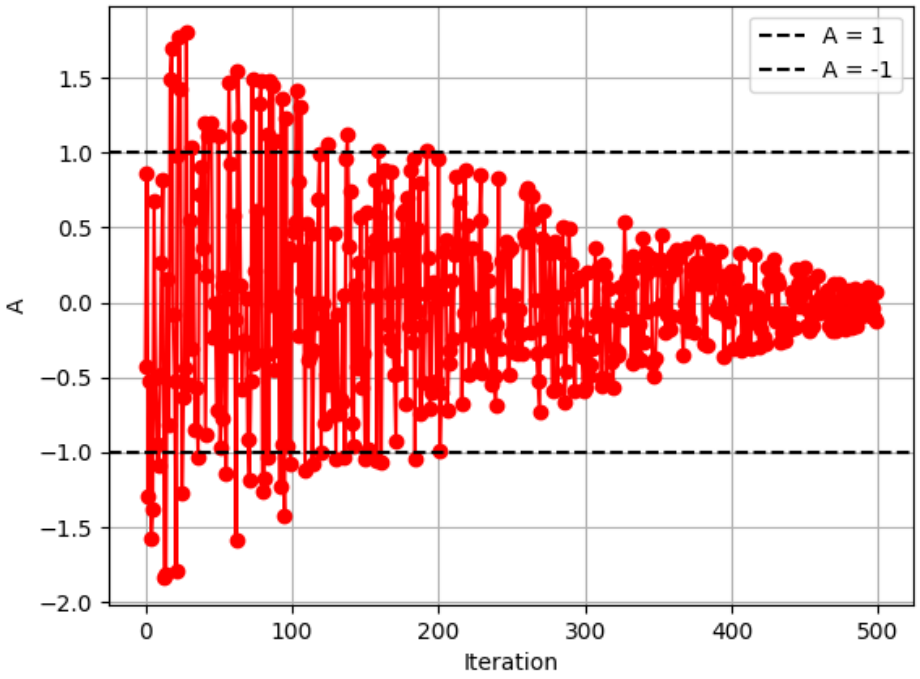

Figure 3.19: The distribution of A for the quadratic decrease of a

For this modification, a random experiment with 500 iterations showed that $|A| < 1$ for 444 instances, while $|A| > 1$ for the remaining 56 as shown in figure 3.19. The performance of this modification is shown in figure 3.20 and 3.21

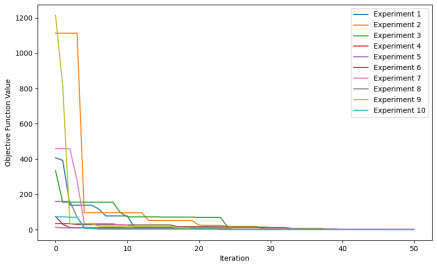

(a) Sphere function

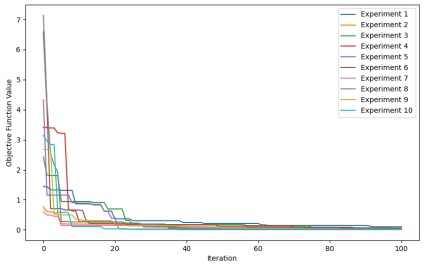

(b) Sum of absolutes

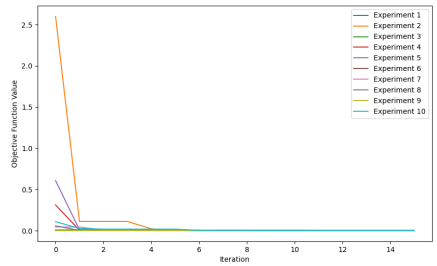

(c) Sum of squares

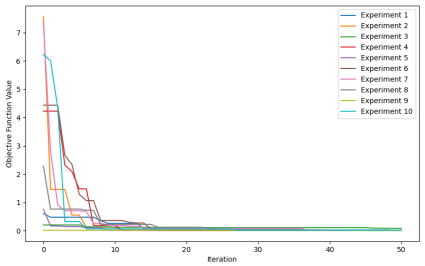

(d) Rosenbrock function

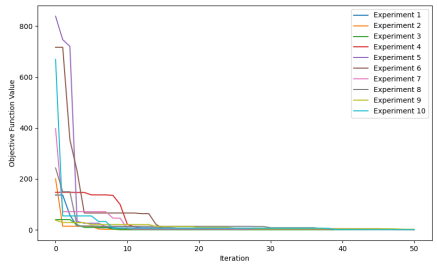

(e) Step function

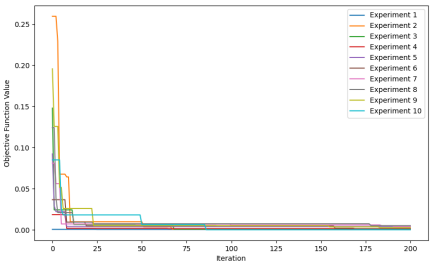

(f) Quartic function (with noise)

Figure 3.20: Performance of the quadratic decrease variation on uni-modal benchmark functions

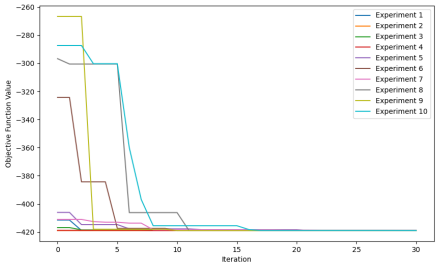

(a) Schwefel function

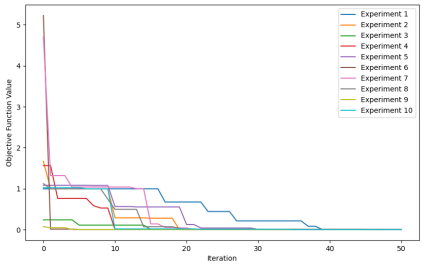

(b) Rastrigin function

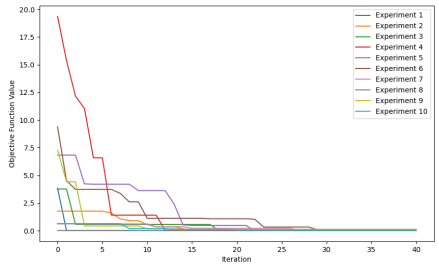

(c) Ackley function

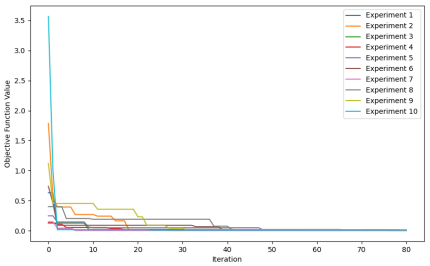

(d) Griewank function

Figure 3.21: Performance of the quadratic decrease variation on multi-modal benchmark functions

In terms of solution quality, the modification showed a slightly weaker performance on the benchmark functions, evidenced by a higher chance of getting stuck in local minima for a few unimodal functions as shown in figure 3.20b and figure 3.20a. As expected, convergence was quick in most cases, with the longest benchmark taking 40 iterations to converge. Due to the higher exploitation bias, the modification performed considerably weaker for the quartic function (with noise) as shown in figure 3.20f where only one of the 10 experiments converged to near-zero. As for the other multimodal functions, the modification still managed to escape local minima but this is solely a result of the efficacy of the IWOA and its improved search strategy. Nevertheless, the increased exploitation likelihood can still be seen, compared with other exploratory modifications. The statistical performance is shown in table 3.7.

Table 3.7: Statistical overview for the quadratically decreasing variation's performance on benchmark functions

Function	**Domain range**	**Global Minimum**	**Epochs**	**Dimension**	**Mean of last fitness**	**Std. dev. of last fitness**
Sphere	(-100, 100)	0	500	2	4.9452×10^{-4}	5.8251×10^{-4}
Sum of absolute values	(-10, 10)	0	500	2	9.8680×10^{-4}	1.1593×10^{-3}
Sum of squares	(-10, 10)	0	500	2	8.32×10^{-10}	1.54×10^{-9}
Rosenbrock	(-2.048, 2.048)	0	500	2	7.13×10^{-5}	1.0248×10^{-4}
Step	(-100, 100)	0	500	2	1.8734×10^{-3}	3.8821×10^{-3}
Quartic (with noise)	(-1.28, 1.28)	0	500	9	6.0907×10^{-2}	6.8556×10^{-2}
Schwefel	(-500, 500)	418.9829	500	1	4.1898×10^{2}	1.41×10^{-6}
Rastrigin	(-5.12, 5.12)	0	500	2	7.1003×10^{-4}	1.5587×10^{-3}
Ackley	(-32, 32)	0	500	2	1.5653×10^{-2}	1.3175×10^{-2}
Griewank	(-600, 600)	0	500	2	3.2023×10^{-2}	2.8009×10^{-2}

3.6.2 Logarithmic Variation

For this variation, we adopt the log function shown in Equation 3.30 as a non-linear way to decrease the parameter a as the iterations proceed. Initially, the log term will always equal to 0 for any positive number of iterations ($\max_{\text{iter}} > 1$), such that $a = 2$ at first.

$$a = 2 - \log_{\max_{\text{iter}}}(i + 1) \tag{3.30}$$

Apart from the non-linear and stepwise manner in which the log function generally decelerates, it's important to note that the 'base' of the logarithmic function (which is the maximum number of iterations in this case) is a key setting that will slow down the pace at which a descends. This is because the higher the base ($\max_{\text{iter}}$) is, the slower the pace at which a descends will be. This holds as more significant changes in i will be needed to cause the same amount of change in a.

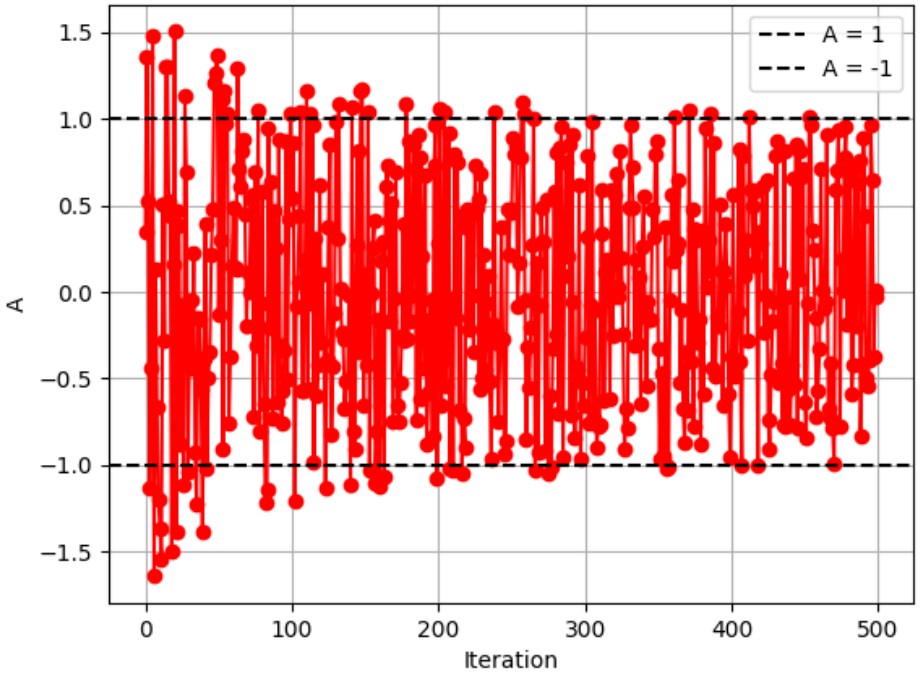

Figure 3.22: The distribution of A for the logarithmic decrease of a

As shown in figure 3.22, for 500 iterations of $|A|$, 67 points lay above 1, while the remaining 433 lay below 1. This demonstrates a higher propensity towards exploitation by the algorithm with this modification. Moreover, it can be seen that for the first 20% of iterations, more of the points where $|A|$ is above 1, are concentrated. This is a result of the logarithmic property of a.

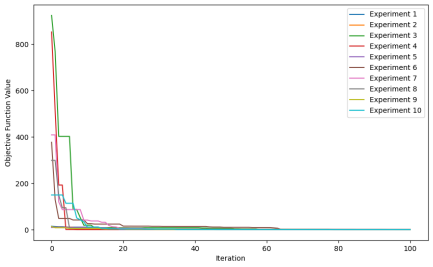

(a) Sphere function

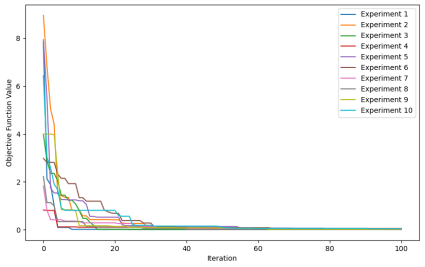

(b) Sum of absolutes

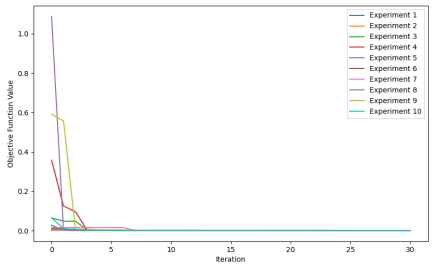

(c) Sum of squares

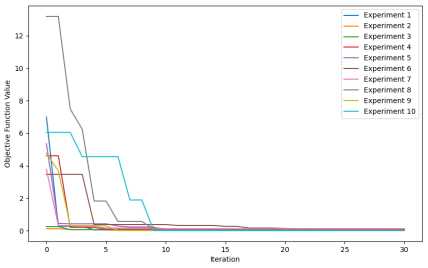

(d) Rosenbrock function

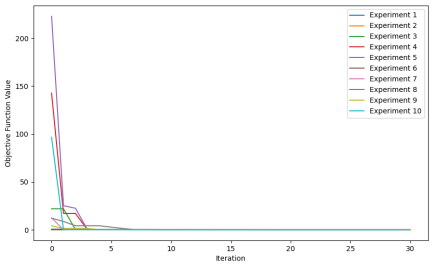

(e) Step function

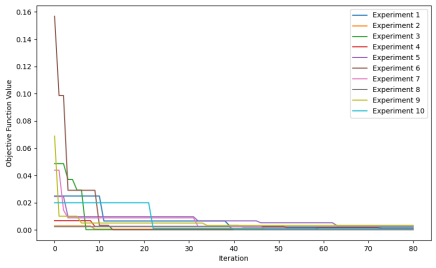

(f) Quartic function (with noise)

Figure 3.23: Performance of the logarithmic decrease variation on uni-modal benchmark functions

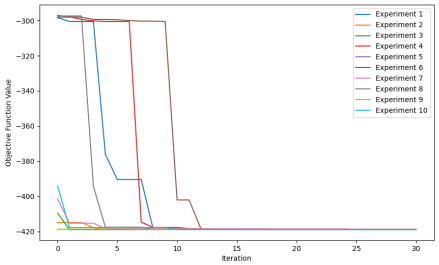

(a) Schwefel function

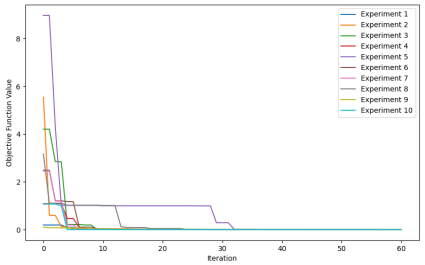

(b) Rastrigin function

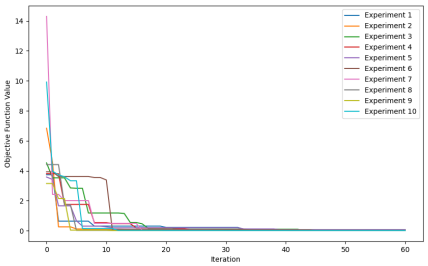

(c) Ackley function

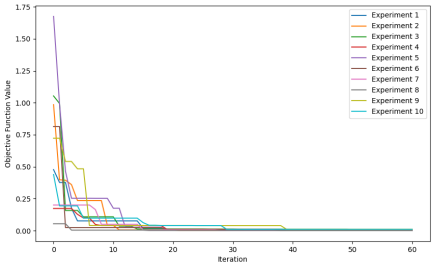

(d) Griewank function

Figure 3.24: Performance of the logarithmic variation on multi-modal benchmark functions

The benchmark tests on the log variation revealed a more sluggish convergence speed towards the global minimum. This is expected due to the high exploitation likelihood of the algorithm as a result of the modification. The algorithm was noticed to use two or three iterations to move past a current fitness or position when dealing with unimodal benchmarks as shown in figures 3.23b and 3.23d in particular. This effect was greatly increased when handling multimodal benchmark solutions such as the Schwefel and Ackley functions as shown in figures 3.24a and 3.24c respectively. While eventual convergence did occur, the noted inefficiency of this modification may create additional computation requirements when applied to various practical problems. The logarithmic variation may not be the most effective exploitation modification for cases with a maximum iteration count too high. Table 3.8 highlights the statistical performance of the modification.

Table 3.8: Statistical overview of the logarithmic variation's performance on benchmark functions

Function	**Domain range**	**Global Minimum**	**Epochs**	**Dimension**	**Mean of last fitness**	**Std. dev. of last fitness**
Sphere	(-100, 100)	0	500	2	2.3071×10^{-4}	2.6457×10^{-4}
Sum of absolute values	(-10, 10)	0	500	2	1.1128×10^{-3}	1.0178×10^{-3}
Sum of squares	(-10, 10)	0	500	2	9.91×10^{-10}	1.12×10^{-9}
Rosenbrock	(-2.048, 2.048)	0	500	2	5.68×10^{-5}	1.0487×10^{-4}
Step	(-100, 100)	0	500	2	4.7594×10^{-4}	7.0928×10^{-4}
Quartic (with noise)	(-1.28, 1.28)	0	500	9	3.7805×10^{-2}	1.2056×10^{-2}
Schwefel	(-500, 500)	418.9829	500	1	4.1898×10^{2}	6.48×10^{-7}
Rastrigin	(-5.12, 5.12)	0	500	2	6.8722×10^{-4}	1.6527×10^{-3}
Ackley	(-32, 32)	0	500	2	1.2142×10^{-2}	1.0360×10^{-2}
Griewank	(-600, 600)	0	500	2	4.4344×10^{-2}	3.7551×10^{-2}

3.7 Evaluation Criteria

To extract the parameters from the previously discussed PV models from the I-V dataset, whatever optimization technique is being used needs a function to define the objective of the system before it discovers a way to optimize it properly. In previous studies, the root-mean-square error [43] is vastly engaged to describe the objective function by showing how far off the estimated values of the current is, from what has been recorded or measured. This error is the algorithm's fitness function and is described as follows:

$$\mathbf{min}F(x) = \mathbf{RMSE}(x) = \sqrt{\frac{1}{N_E} \cdot \sum_{i=1}^{N_E} f_k(V_t, I_t, \Phi)^2} \tag{3.31}$$

where N_E is the number of samples of experimental data, and Φ is the decision vector of the parameters to be computed. For the research case which will be on the triple diode model, Φ will be the vector-array (R_s, R_{sh}, I_{ph}, I_{sd1}, I_{sd2}, I_{sd3}, n_1, n_2 and n_3). The modifications will be employed to minimize this function.

Chapter 4

Results

The final procedure involved taking a sample measurement from the experimental methods described in Table 4 from the paper on the IWOA by Khanna et al. [52]. The idea was to attempt to replicate the experiment, using all the data variables from the previous research as pseudo-control variables such that the effect of the modifications can be examined more comparatively. The final application was attempted using Python 3.11.2 [78] on the same system specifications disclosed above in the section on Exploratory Modification.

In an attempt to generate an I-V curve using the data sample, a range of continuous voltage values was first defined which spanned from 0 volts to a value just beyond the open-circuit voltage of the module being modelled. Next, a 'triple-diode-model' function modelled after equation 3.6 was defined using Python's Scipy library [97] and used to calculate the corresponding current (I) based on the set of data variables collected from Khanna et al.'s research. The same variable bounds for each of the parameters were declared as a list of tuples with each tuple containing the bounds of each variable to be estimated. The temperature was set to STC at 330 degrees Kelvin. The final step was for the set of current values and the matplotlib python library [94] to be used to plot and generate the I-V curve which the modified IWOA will attempt to calculate. Unfortunately, this led to unforeseen limitations which were not resolvable given the research time frame and hence did not allow the final experimental phase of the thesis to be executed. However, pre-experiment results show a good possibility of improved parameter esti-

mation for triple-diode models and a way to measurably tune the bias of the algorithm. The repository to these methods has been referenced in this thesis [3]

Chapter 5

Conclusions and future work

In this thesis, six modifications to the coefficient A in the improved whale algorithm were proposed to improve its parameter extraction performance. Two of the six modifications leveraged algebraic functions while the remaining 4 adopted transcendental functions. The functions were plotted and tested using ten benchmark functions. The modifications were shown to sustain the feasibility of the algorithm as an optimizer while providing measurable adjustments to the algorithm's exploration-exploitation balance. In future work, the effect of the modifications to the parameter estimation of triple-diode photovoltaic models will be investigated in full.

Bibliography

[1] Abbassi, R., Abbassi, A., Heidari, A. A. and Mirjalili, S. [2019], 'An efficient salp swarm-inspired algorithm for parameters identification of photovoltaic cell models', *Energy conversion and management* **179**, 362–372.

[2] Ahmad, T., Sobhan, S. and Nayan, M. F. [2016], 'Comparative analysis between single diode and double diode model of pv cell: concentrate different parameters effect on its efficiency', *Journal of power and Energy Engineering* **4**(3), 31–46.

[3] Ajetunmobi, O. [2023], 'Improved parameter estimation of triple diode photovoltaic models', https://github.com/Shegzimus/Improved-Parameter-Estimation-of-Triple-Diode-Photovoltaic-Models. Accessed: 28/02/2024.

[4] Akhil, S., Akash, S., Pasha, A., Kulkarni, B., Jalalah, M., Alsaiari, M., Harraz, F. A. and Balakrishna, R. G. [2021], 'Review on perovskite silicon tandem solar cells: Status and prospects 2t, 3t and 4t for real world conditions', *Materials & Design* **211**, 110138.

[5] Aoun, N., Chenni, R., Nahman, B. and Bouchouicha, K. [2014], 'Evaluation and validation of equivalent five-parameter model performance for photovoltaic panels using only reference data', *Energy and Power Engineering* **06**, 235–245.
URL: *https://api.semanticscholar.org/CorpusID:47002686*

[6] Atwater, H. A. [2012], Full spectrum boosts solar cell power.
URL: *https://api.semanticscholar.org/CorpusID:135450358*

[7] Azzouzi, M., Popescu, D. and Bouchahdane, M. [2016], 'Modeling of electrical characteristics of photovoltaic cell considering single-diode model', *Journal of Clean Energy Technologies* **4**(6), 414–420.

[8] Bäck, T. [n.d.], Artificial landscapes, *in* 'Evolutionary Algorithms in Theory and Practice', Oxford University Press.

[9] Bastidas-Rodriguez, J. D., Petrone, G., Ramos-Paja, C. A. and Spagnuolo, G. [2017], 'A genetic algorithm for identifying the single diode model parameters of a photovoltaic panel', *Mathematics and Computers in Simulation* **131**, 38–54.

[10] Belhachat, F. and Larbes, C. [2019], 'Comprehensive review on global maximum power point tracking techniques for pv systems subjected to partial shading conditions', *Solar Energy* **183**, 476–500.

[11] Bhukya, L., Kedika, N. and Salkuti, S. R. [2022], 'Enhanced maximum power point techniques for solar photovoltaic system under uniform insolation and partial shading conditions: A review', *Algorithms* **15**, 365.

[12] Bäck, T. and Schwefel, H.-P. [1993], 'An overview of evolutionary algorithms for parameter optimization', *Evolutionary Computation* **1**(1), 1–23.

[13] C, C., Taha, Shaji, M., Y, R. R., Jawwad, M. and Sharma, G. [2019], 'A novel optimization method for parameter extraction of industrial solar cells', *2019 Innovations in Power and Advanced Computing Technologies (i-PACT)* **1**, 1–6.
URL: *https://api.semanticscholar.org/CorpusID:210697813*

[14] Changmai, P., Deka, S., Kumar, S., Babu, T. S., Aljafari, B. and Nastasi, B. [2022], 'A critical review on the estimation techniques of the solar pv cell's unknown parameters', *Energies* .
URL: *https://api.semanticscholar.org/CorpusID:252774230*

[15] Charfi, W., Chaabane, M., Mhiri, H. and Bournot, P. [2018], 'Performance evaluation of a solar photovoltaic system', *Energy Reports* **4**, 400–406.

[16] Charles, J., Abdelkrim, M., Muoy, Y. and Mialhe, P. [1981], 'A practical method of analysis of the current-voltage characteristics of solar cells', *Solar cells* **4**(2), 169–178.

[17] Chin, V. J., Salam, Z. and Ishaque, K. [2015], 'Cell modelling and model parameters estimation techniques for photovoltaic simulator application: A review', *Applied Energy* **154**, 500–519.

[18] Ciulla, G., Brano, V. L., Di Dio, V. and Cipriani, G. [2014], 'A comparison of different one-diode models for the representation of i–v characteristic of a pv cell', *Renewable and Sustainable Energy Reviews* **32**, 684–696.

[19] Cubas, J., Pindado, S. and Farrahi, A. [2013], New method for analytical photovoltaic parameter extraction, *in* '2013 International Conference on Renewable Energy Research and Applications (ICRERA)', IEEE, pp. 873–877.

[20] De Soto, W., Klein, S. A. and Beckman, W. A. [2006], 'Improvement and validation of a model for photovoltaic array performance', *Solar energy* **80**(1), 78–88.

[21] Digalakis, J. G. and Margaritis, K. G. [2001], 'On benchmarking functions for genetic algorithms', *International journal of computer mathematics* **77**(4), 481–506.

[22] Ding, L. C., Akbarzadeh, A. and Tan, L. [2018], 'A review of power generation with thermoelectric system and its alternative with solar ponds', *Renewable and sustainable energy reviews* **81**, 799–812.

[23] Dixon, L. and Mills, D. [1994], 'Effect of rounding errors on the variable metric method', *Journal of Optimization Theory and Applications* **80**(1), 175–179.

[24] Dokshin, F. A., Gherghina, M. and Thiede, B. C. [2024], 'Closing the green gap? changing disparities in residential solar installation and the importance of regional heterogeneity', *Energy Research & Social Science* **107**, 103338.

[25] Donovan, M. D., Bourne, B. and de Roche, J. T. [2010], 'Efficiency vs. irradiance characterization of pv modules requires angle-of-incidence and spectral corrections', *2010 35th IEEE Photovoltaic Specialists Conference* pp. 002301–002305.
URL: *https://api.semanticscholar.org/CorpusID:22555395*

[26] Easwarakhanthan, T., Bottin, J., Bouhouch, I. and Boutrit, C. [1986], 'Nonlinear minimization algorithm for determining the solar cell parameters with microcomputers', *International journal of solar energy* **4**(1), 1–12.

[27] Elazab, O. S., Hasanien, H. M., Elgendy, M. A. and Abdeen, A. M. [2018], 'Parameters estimation of single-and multiple-diode photovoltaic

model using whale optimisation algorithm', *IET Renewable Power Generation* **12**(15), 1755–1761.

[28] Elsheikh, A. H., Sharshir, S. W., Ali, M. K. A., Shaibo, J., Edreis, E. M., Abdelhamid, T., Du, C. and Haiou, Z. [2019], 'Thin film technology for solar steam generation: A new dawn', *Solar Energy* **177**, 561–575.

[29] Et-torabi, K., Nassar-eddine, I., Obbadi, A., Errami, Y., Rmaily, R., Sahnoun, S., Fajri, A. E. and Agunaou, M. [2017], 'Parameters estimation of the single and double diode photovoltaic models using a gauss–seidel algorithm and analytical method: A comparative study', *Energy Conversion and Management* **148**, 1041–1054.
URL: *https://api.semanticscholar.org/CorpusID:117133421*

[30] Fathy, A. and Rezk, H. [2017], 'Parameter estimation of photovoltaic system using imperialist competitive algorithm', *Renewable Energy* **111**, 307–320.

[31] Floudas, C. A., Pardalos, P. M., Adjiman, C., Esposito, W. R., Gümüs, Z. H., Harding, S. T., Klepeis, J. L., Meyer, C. A. and Schweiger, C. A. [2013], *Handbook of test problems in local and global optimization*, Vol. 33, Springer Science & Business Media.

[32] Fuchs, D. and Sigmund, H. [1986], 'Analysis of the current-voltage characteristic of solar cells', *Solid-state electronics* **29**(8), 791–795.

[33] Gao, S., Wang, K., Tao, S., Jin, T., Dai, H. and Cheng, J. [2021], 'A state-of-the-art differential evolution algorithm for parameter estimation of solar photovoltaic models', *Energy Conversion and Management* **230**, 113784.

[34] Gow, J. and Manning, C. [1999], 'Development of a photovoltaic array model for use in power-electronics simulation studies', *IEE Proceedings-Electric Power Applications* **146**(2), 193–200.

[35] Guo, L., Meng, Z., Sun, Y. and Wang, L. [2016], 'Parameter identification and sensitivity analysis of solar cell models with cat swarm optimization algorithm', *Energy Conversion and Management* **108**, 520–528.
URL: *https://api.semanticscholar.org/CorpusID:110591973*

[36] Gupta, S. and Saurabh, K. [2017*a*], Modified artificial killer whale optimization algorithm for maximum power point tracking under partial shading condition, *in* '2017 International Conference on Recent Trends

in Electrical, Electronics and Computing Technologies (ICRTEECT)', IEEE, pp. 87–92.

[37] Gupta, S. and Saurabh, K. [2017*b*], Modified artificial wolf pack method for maximum power point tracking under partial shading condition, *in* '2017 International Conference on Power and Embedded Drive Control (ICPEDC)', IEEE, pp. 60–65.

[38] Gupta, S., Tiwari, H., Fozdar, M. and Chandna, V. [2012], Development of a two diode model for photovoltaic modules suitable for use in simulation studies, *in* '2012 Asia-Pacific Power and Energy Engineering Conference', IEEE, pp. 1–4.

[39] Hajek, B. [1985], A tutorial survey of theory and applications of simulated annealing, *in* '1985 24th IEEE Conference on Decision and Control', IEEE, pp. 755–760.

[40] Hao, P. and Zhang, Y. [2021], 'An improved method for parameter identification and performance estimation of pv modules from manufacturer datasheet based on temperature-dependent single-diode model', *IEEE Journal of Photovoltaics* **11**, 1446–1457.
URL: *https://api.semanticscholar.org/CorpusID:239041159*

[41] Harnock, J. I. [2007], Frameless photovoltaic module.
URL: *https://api.semanticscholar.org/CorpusID:141367946*

[42] Hasanien, H. M. [2018], 'Performance improvement of photovoltaic power systems using an optimal control strategy based on whale optimization algorithm', *Electric Power Systems Research* **157**, 168–176.

[43] Ishaque, K., Salam, Z., Mekhilef, S. and Shamsudin, A. [2012], 'Parameter extraction of solar photovoltaic modules using penalty-based differential evolution', *Applied Energy* **99**, 297–308.

[44] Jain, A. and Kapoor, A. [2004], 'Exact analytical solutions of the parameters of real solar cells using lambert w-function', *Solar Energy Materials and Solar Cells* **81**(2), 269–277.

[45] Jordehi, A. R. [2016], 'Parameter estimation of solar photovoltaic (pv) cells: A review', *Renewable and Sustainable Energy Reviews* **61**, 354–371.

[46] Jordehi, A. R. [2018], 'Enhanced leader particle swarm optimisation (elpso): An efficient algorithm for parameter estimation of photovoltaic (pv) cells and modules', *Solar Energy* **159**, 78–87.

[47] Kabir, E., Kumar, P., Kumar, S., Adelodun, A. A. and Kim, K.-H. [2018], 'Solar energy: Potential and future prospects', *Renewable and Sustainable Energy Reviews* **82**, 894–900.

[48] Kaldellis, J., Spyropoulos, G., Kavadias, K. and Koronaki, I. [2009], 'Experimental validation of autonomous pv-based water pumping system optimum sizing', *Renewable Energy* **34**(4), 1106–1113.

[49] Karaboga, D. [2010], 'Artificial bee colony algorithm', *scholarpedia* **5**(3), 6915.

[50] Kebir, S. T., Cheikh, M. S. A. and Haddadi, M. [2018], 'A set of smart swarm-based optimization algorithms applied for determining solar photovoltaic cell's parameters', *Renewable Energy for Smart and Sustainable Cities* .
URL: *https://api.semanticscholar.org/CorpusID:69716100*

[51] Khanna, V., Das, B., Bisht, D., Singh, P. et al. [2015*a*], 'A three diode model for industrial solar cells and estimation of solar cell parameters using pso algorithm', *Renewable Energy* **78**, 105–113.

[52] Khanna, V., Das, B., Bisht, D., Singh, P. et al. [2015*b*], 'A three diode model for industrial solar cells and estimation of solar cell parameters using pso algorithm', *Renewable Energy* **78**, 105–113.

[53] Khanna, V., Das, B. K., Bisht, D. C. S., Vandana and Singh, P. K. [2014], Estimation of photovoltaic cells model parameters using particle swarm optimization.
URL: *https://api.semanticscholar.org/CorpusID:117185206*

[54] Kumar, C. S. and Rao, R. S. [2016], 'A novel global mpp tracking of photovoltaic system based on whale optimization algorithm', *International Journal of Renewable Energy Development* **5**(3), 225–232.

[55] Lang, Z. and Zhang, Y. [2020], 'Parameter identification and performance estimation for pv modules based on reduced forms model', *Journal of Renewable and Sustainable Energy* .
URL: *https://api.semanticscholar.org/CorpusID:224965526*

[56] Laudani, A., Fulginei, F. R. and Salvini, A. [2014], 'High performing extraction procedure for the one-diode model of a photovoltaic panel from experimental i–v curves by using reduced forms', *Solar Energy* **103**, 316–326.

[57] Lineykin, S., Averbukh, M. and Kuperman, A. [2012], Five-parameter model of photovoltaic cell based on stc data and dimensionless, *in* '2012 IEEE 27th Convention of Electrical and Electronics Engineers in Israel', IEEE, pp. 1–5.

[58] Lineykin, S., Averbukh, M. and Kuperman, A. [2014], 'An improved approach to extract the single-diode equivalent circuit parameters of a photovoltaic cell/panel', *Renewable and Sustainable Energy Reviews* **30**, 282–289.

[59] Luo, J. and Shi, B. [2019], 'A hybrid whale optimization algorithm based on modified differential evolution for global optimization problems', *Applied Intelligence* **49**, 1982–2000.

[60] Margolis, R. and Zuboy, J. [n.d.], 'Nontechnical barriers to solar energy use: Review of recent literature'.
URL: *https://www.osti.gov/biblio/893639*

[61] Marion, B., Anderberg, A., Deline, C., del Cueto, J. A., Muller, M., Perrin, G., Rodriguez, J., Rummel, S. R., Silverman, T. J., Vignola, F., Kessler, R., Peterson, J., Barkaszi, S. F., Jacobs, M., Riedel, N., Pratt, L. and King, B. H. [2014], 'New data set for validating pv module performance models', *2014 IEEE 40th Photovoltaic Specialist Conference (PVSC)* pp. 1362–1366.
URL: *https://api.semanticscholar.org/CorpusID:8608001*

[62] Melvin, A. [2017], Open circuit voltage calculation using temperature and irradiance.
URL: *https://api.semanticscholar.org/CorpusID:70296782*

[63] Messaoud, R. B. [2019], 'Extraction of uncertain parameters of double-diode model of a photovoltaic panel using simulated annealing optimization', *The Journal of Physical Chemistry C* .
URL: *https://api.semanticscholar.org/CorpusID:209711488*

[64] Mirjalili, S. and Lewis, A. [2016], 'The whale optimization algorithm', *Advances in engineering software* **95**, 51–67.

[65] Mohamed, S. A. E., Mageed, H. M. A., Ahmed, W. A. and Saleh, A. A. [2020], 'Estimate the parameters of photovoltaic module by fodpso', *International journal of engineering research and technology* **9**.
URL: *https://api.semanticscholar.org/CorpusID:221567068*

[66] Mohapatra, A. [2018], Optimized parameter estimation, array configuration and mppt control of standalone photovoltaic system.
URL: *https://api.semanticscholar.org/CorpusID:69846355*

[67] Mohapatra, A., Nayak, B. and Mohanty, K. B. [2018], 'Parameter estimation of single diode pv module based on nelder-mead optimization algorithm', *World Journal of Engineering* **15**, 00–00.
URL: *https://api.semanticscholar.org/CorpusID:125545436*

[68] Molga, M. and Smutnicki, C. [2005], 'Test functions for optimization needs', *Test functions for optimization needs* **101**, 48.

[69] Mughal, M. A., Ma, Q. and Xiao, C. [2017], 'Photovoltaic cell parameter estimation using hybrid particle swarm optimization and simulated annealing', *Energies* **10**(8), 1213.

[70] Nasa [2018], Flexible solar cells.
URL: *https://api.semanticscholar.org/CorpusID:224344376*

[71] Nichinte, A. S., Vyawahare, V. A. and Magare, D. B. [2020], 'Estimation and comparison of module temperature model coefficient for different pv technology module', *2020 3rd International Conference on Communication System, Computing and IT Applications (CSCITA)* pp. 13–17.
URL: *https://api.semanticscholar.org/CorpusID:220568644*

[72] Niu, Q., Zhang, L. and Li, K. [2014], 'A biogeography-based optimization algorithm with mutation strategies for model parameter estimation of solar and fuel cells', *Energy conversion and management* **86**, 1173–1185.

[73] Olanipekun, M. U., Olanipekun, A. J., Amusa, K. A. and Opeodu, A. J. [2018], Parameters extraction of a double-diode model of photovoltaic cell using newton-raphson method.
URL: *https://api.semanticscholar.org/CorpusID:214668467*

[74] Oliva, D., Abd Elaziz, M., Elsheikh, A. H. and Ewees, A. A. [2019], 'A review on meta-heuristics methods for estimating parameters of solar cells', *Journal of Power Sources* **435**, 126683.

[75] Panua, R. and Moyra, T. [2012], Building integrated photovoltaic (bipv) system.
URL: *https://api.semanticscholar.org/CorpusID:108089448*

[76] Parida, B., Iniyan, S. and Goic, R. [2011], 'A review of solar photovoltaic technologies', *Renewable and sustainable energy reviews* **15**(3), 1625–1636.

[77] Purohit, I. and Purohit, P. [2017], 'Technical and economic potential of concentrating solar thermal power generation in india', *Renewable and Sustainable Energy Reviews* **78**, 648–667.

[78] Python Software Foundation [2023], 'Python 3.11 documentation', https://docs.python.org/3.11/. Accessed: 28/04/2024.

[79] Quaschning, V. and Hanitsch, R. [1996], 'Numerical simulation of current-voltage characteristics of photovoltaic systems with shaded solar cells', *Solar energy* **56**(6), 513–520.

[80] Rajesh, R. and Mabel, M. C. [2015], 'A comprehensive review of photovoltaic systems', *Renewable and sustainable energy reviews* **51**, 231–248.

[81] Ramspeck, K., Bothe, K., Hinken, D., Fischer, B., Schmidt, J. and Brendel, R. [2007], 'Recombination current and series resistance imaging of solar cells by combined luminescence and lock-in thermography', *Applied Physics Letters* **90**(15).

[82] Rana, N., Latiff, M. S. A., Abdulhamid, S. M. and Chiroma, H. [2020], 'Whale optimization algorithm: a systematic review of contemporary applications, modifications and developments', *Neural Computing and Applications* **32**, 16245–16277.

[83] Rastrigin, L. A. [1974], 'Systems of extremal control', *Nauka* .

[84] Rezk, H. and Abdelkareem, M. [2021], 'Optimal parameter identification of triple diode model for solar photovoltaic panel and cells', *Energy Reports* **8**.

[85] Rodriguez, C. and Amaratunga, G. A. J. [2007], 'Analytic solution to the photovoltaic maximum power point problem', *IEEE Transactions on Circuits and Systems I: Regular Papers* **54**(9), 2054–2060.

[86] Saad, M. and Kassis, A. [2003], 'Effect of interface recombination on solar cell parameters', *Solar energy materials and solar cells* **79**(4), 507–517.

[87] Saurabh, K. and Gupta, S. [2017], Modified artificial killer whale optimization for optimal power flow, *in* '2017 8th International Conference on Computing, Communication and Networking Technologies (ICCCNT)', IEEE, pp. 1–7.

[88] Sera, D., Teodorescu, R. and Rodriguez, P. [2007], Pv panel model based on datasheet values, *in* '2007 IEEE international symposium on industrial electronics', IEEE, pp. 2392–2396.

[89] Sheikh, N. J., Kocaoglu, D. F. and Lutzenhiser, L. [2016], 'Social and political impacts of renewable energy: Literature review', *Technological Forecasting and Social Change* **108**, 102–110.

[90] Shi, Y., Zhu, W., Xiang, Y. and Feng, Q. [2020], 'Condition-based maintenance optimization for multi-component systems subject to a system reliability requirement', *Reliab. Eng. Syst. Saf.* **202**, 107042.
URL: *https://api.semanticscholar.org/CorpusID:219746025*

[91] So, J. H., Yu, B. G., Hwang, H. M., Yu, G. J. and Ahn, S. J. [2008], 'Performance estimation and evaluation of residential grid-connected pv system', *2008 33rd IEEE Photovoltaic Specialists Conference* pp. 1–4.
URL: *https://api.semanticscholar.org/CorpusID:25609433*

[92] Soliman, M. A., Hasanien, H. M. and Alkuhayli, A. [2020], 'Marine predators algorithm for parameters identification of triple-diode photovoltaic models', *IEEE Access* **8**, 155832–155842.

[93] *The Effect of Irradiance and Temperature on the Performance of Photovoltaic Modules* [2017].
URL: *https://api.semanticscholar.org/CorpusID:213195148*

[94] Tosi, S. [2009], *Matplotlib for Python developers*, Packt Publishing Ltd.

[95] Tvingstedt, K., Gil-Escrig, L., Momblona, C., Rieder, P., Kiermasch, D., Sessolo, M., Baumann, A., Bolink, H. J. and Dyakonov, V. [2017], 'Removing leakage and surface recombination in planar perovskite solar cells', *ACS Energy Letters* **2**(2), 424–430.

[96] Vikhar, P. A. [2016], Evolutionary algorithms: A critical review and its future prospects, *in* '2016 International Conference on Global Trends in Signal Processing, Information Computing and Communication (ICGTSPICC)', pp. 261–265.

[97] Virtanen, P., Gommers, R., Oliphant, T. E., Haberland, M., Reddy, T., Cournapeau, D., Burovski, E., Peterson, P., Weckesser, W., Bright, J. et al. [2020], 'Scipy 1.0: fundamental algorithms for scientific computing in python', *Nature methods* **17**(3), 261–272.

[98] Wang, D., Tan, D. and Liu, L. [2018], 'Particle swarm optimization algorithm: an overview', *Soft computing* **22**, 387–408.

[99] Wang, L., Chen, Z., Guo, Y., Hu, W., Chang, X., Wu, P., Han, C. and Li, J. [2021], 'Accurate solar cell modeling via genetic neural network-based meta-heuristic algorithms', *Frontiers in Energy Research* **9**, 696204.

[100] Xiong, G., Zhang, J., Shi, D. and He, Y. [2018], 'Parameter extraction of solar photovoltaic models using an improved whale optimization algorithm', *Energy conversion and management* **174**, 388–405.

[101] Yamaguchi, M., Dimroth, F., Geisz, J. F. and Ekins-Daukes, N. J. [2021], 'Multi-junction solar cells paving the way for super high-efficiency', *Journal of Applied Physics* .
URL: *https://api.semanticscholar.org/CorpusID:237878459*

[102] Yang, B., Wang, J., Zhang, X., Yu, T., Yao, W., Shu, H., Zeng, F. and Sun, L. [2020], 'Comprehensive overview of meta-heuristic algorithm applications on pv cell parameter identification', *Energy Conversion and Management* **208**, 112595.

[103] Yang, X.-S. [2010], 'Firefly algorithm, stochastic test functions and design optimisation', *International journal of bio-inspired computation* **2**(2), 78–84.

[104] Yang, X.-S., Karamanoglu, M. and He, X. [2014], 'Flower pollination algorithm: a novel approach for multiobjective optimization', *Engineering optimization* **46**(9), 1222–1237.

[105] Yousri, D., Rezk, H. and Fathy, A. [2020], 'Identifying the parameters of different configurations of photovoltaic models based on recent artificial ecosystem-based optimization approach', *International Journal of Energy Research* **44**(14), 11302–11322.